Sedimentology (2004) **51,** 553–589 doi: 10.1111/j.1365-3091.2004.00636.x

High-arctic fan delta recording deglaciation and environment disequilibrium

IDA LØNNE*[1] and W. NEMEC†
**The University Centre on Svalbard (UNIS), Longyearbyen, Norway*
†*Department of Earth Science, University of Bergen, 5007 Bergen, Norway*

ABSTRACT

Study of a Holocene fan delta in Adventfjorden, Spitsbergen, provides new insight into the nature of high-arctic coastal sedimentation and deglaciation dynamics. The fjord-side, gravelly Gilbert-type fan delta began to form at the local marine limit *c.* 10 ka BP, supplied seasonally with sediment by meltwater from a cirque glacier left behind by the retreating Late Weichselian ice sheet. Relative sea level had fallen by 63 m, and the fan delta reached a radius of *c.* 1 km by 6 ka BP, when the relic glacier eventually melted down and fluvial activity declined. A strong influence of marine processes is recorded by the fan-delta foreset facies, overlain by alluvium. Supplied with sediment by longshore drift, the fan-delta front continued to advance at a lower rate, while relative sea level fell further by 5 m and ceased to fall around 5·4 ka BP. The following transgression was countered by longshore sediment supply until 4·7 ka BP, when the delta-front beach aggraded and a spit platform began to climb onto the delta plain, recording a relative sea-level rise of 4 m. The subsequent regression was initially non-depositional, with the relative sea level falling by > 4 m in 200 years, outpacing fluvial supply, and the re-emerging fan delta being swept by longshore currents. A regressive beach began to form *c.* 4·3 ka BP, while relative sea level gradually reached its present-day position. The feeder braided stream was wandering across the delta plain during this time, but incised once the fan-delta shoreline began to retreat by wave erosion and turned into a receding modern escarpment. The stream has since been adjusting its profile by gradually eroding the pre-existing alluvium and distributing the coarse sediment supplied from catchment slopes by debrisflows and snow avalanches. Modern snowflows have also spread debris onto the abandoned fan surface. The erosional retreat of the fan delta has been accompanied by lateral shoreline accretion on both its sides. The study has important regional implications and demonstrates that Holocene fan deltas can provide a valuable record of the deglaciation history in high-arctic terrains, where glacial deposits are scarcely preserved on land.

Keywords Facies analysis, fjord, forced regression, Gilbert-type fan delta, Holocene, Svalbard, transgression.

INTRODUCTION

The development of alluvial fans in high-arctic regions is controlled by a unique combination of physical conditions, but has been little studied (cf. Bull, 1977; Nilsen & Moore, 1984; Rachocki & Church, 1990). Although the main controlling factors are similar to those acting at lower latitudes, their role and interplay in a polar region are different (Dixon & Abrahams, 1992; French, 1996). For example, the bulk of flowing water derives from the melting of ice, as

[1]Present address: The Natural History Museums and Botanical Garden, University of Oslo, PO Box 1172 Blindern, N-0318 Oslo, Norway (E-mail: ida.lonne @nhm.uio.no)

in lower latitude proglacial and alpine settings, but the melting process of glaciers and permafrost in high-arctic zone is limited to two or three months a year, which renders the runoff ephemeral – more like the situation in the mid-latitude arid and semi-arid regions. However, the runoff is not brief and flashy, unlike that resulting from torrential rains. The rainfall in a polar desert is sparse, and the meltwater yield is a function of the air temperature, rather than of the precipitation rate. Consequently, the importance of high topographic relief is mainly in controlling the distribution of ice masses and the depth of permafrost, and it is the attitude of the mountain slopes and their insolation that are critical.

The rates of weathering and net denudation in high-arctic regions are low. Despite the sparsity of vegetation, the sediment yield from mountain slopes is extremely non-uniform, depending upon the local availability of meltwater. The supply of sediment to the valleys and coastal zone is limited to outwash from glaciers, resedimentation of glacigenic deposits and the wasting of debris from frost-weathered bedrock cliffs. Arctic alluvial sedimentation thus involves streamflow and debrisflow processes, accompanied by rockfall and sporadic snow avalanches (Jahn, 1960, 1967; Rapp, 1960; Åkerman, 1984; Rudberg, 1986, 1988). High-arctic shorelines are pounded by waves, swept by longshore currents and influenced by tides, but the wave action ceases during the winter, when the coastal waters freeze over. The intermittent activity and interplay of the terrestrial and marine processes are best recorded in the development of Holocene alluvial-fan deltas, which reflect both short- and long-term morphodynamic disequilibria and have been subject to remarkable changes. The fan deltas also bear the effects of relative sea-level change accompanying deglaciation.

The specific character of high-arctic coastal sedimentation is illustrated by the present study of a Holocene fan delta in a deglaciated fjord basin in Svalbard, Norwegian Arctic. The case study also demonstrates the significance of high-arctic fan deltas for reconstruction of regional deglaciation history and serves to highlight important differences between the deglaciation dynamics of high- and mid-latitude regions, as pointed out by recent investigations in Svalbard (Lysså & Lønne, 2001; Sletten *et al.*, 2001). First, the Late Weichselian ice sheet retreated quickly, by calving, from the Svalbard shelf and fjords, but its recession on land was very gradual, leaving behind isolated glaciers. The isolated temperate glaciers melted slowly, driving subglacial erosion and proglacial sedimentation on a seasonal basis, and eventually turning into cold-based ice bodies that melted at an even slower rate. Secondly, the release of water from these local glaciers and the permafrost active layer was incremental, persisting as a seasonal phenomenon over a long time. The active layer has acted as a rechargeable source of meltwater, and also the volume of glaciers fluctuated and might have increased significantly, as during the Little Ice Age (see references above). Thirdly, the ice sheet left sparse subglacial till and few terrestrial moraines, typically ice-cored, and the preservation potential of these deposits is low.

Unlike at mid-latitudes, the deglaciation of a high-arctic terrain is thus slow and highly non-uniform. The transitional 'paraglacial' conditions (Church & Ryder, 1972) in such a climatic setting still involve mainly meltwater, and their duration is greatly extended, whereas the glacial sedimentary record is largely erased. The reconstruction of regional deglaciation history then becomes a formidable task. For example, the scarcity of onshore glacial deposits misled a few generations of geologists into believing that the western coasts and shelf of Svalbard were never covered by ice during the last glacial maximum, and that the westward advance of the Late Weichselian ice sheet was mainly limited to valleys and fjord heads (see review

Fig. 1. (A) Location of the study area in central Spitsbergen, the main island of the arctic Svalbard archipelago (inset), and a topographic map of the Adventfjorden area showing the Hiorthfjellet fan delta and its coastal catchment (dashed outline). The arrows on Platåberget indicate the local direction of meltwater flow at the beginning of fjord deglaciation. Note the local marine limit at *c.* 70 m and the asterisk indicating the location of radiocarbon sample T-11575 (Table 1). (B) Oblique aerial photograph of the Hiorthfjellet fan delta and its high-relief catchment in 1936 (Norwegian Polar Institute, S36-3956). The fan-delta area is divided into three sectors: 1 – the fan delta at its original maximum extent; 2 – its incised active sector; and 3 – the area dominated by modern snow avalanches. The catchment sectors I and II are slope recesses, divided into segments *a* and *b* and merging in segment *c*; segment *d* is the fan-delta head zone. Note the raised wave-cut escarpment and the modern shoreline escarpment passing eastwards into a spit sheltering an intertidal lagoon.

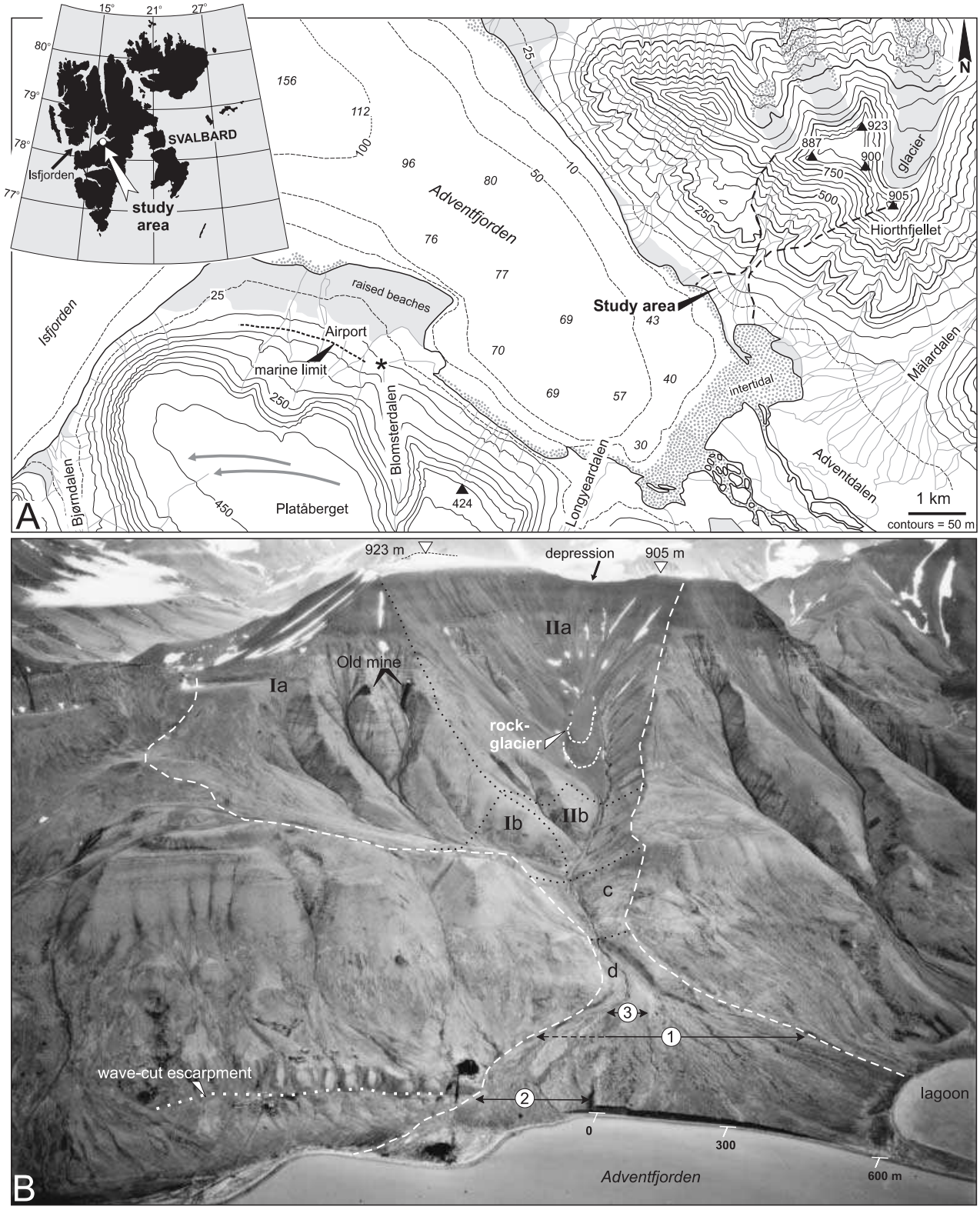

by Landvik *et al.*, 1998). An important aspect of the present study is to demonstrate that a valuable, high-resolution proxy record of deglaciation history can be deciphered from the evolution of high-arctic coastal catchments and associated fan deltas.

THE STUDY AREA

Deglaciation and relative sea level

Svalbard is a high-arctic archipelago (Fig. 1A, inset) located near the western edge of the Barents Sea Shelf, a region repeatedly covered by ice sheets during the Late Pleistocene (Mangerud *et al.*, 1998; Vorren *et al.*, 1998). The last was the Late Weichselian ice sheet, which reached the shelf edge around 18–20 ka BP (Landvik *et al.*, 1998) and began to retreat a few thousand years later. From the modelling of post-glacial crustal rebound, the ice sheet is estimated to have been at least 3000 m thick in the central part of the Barents Sea Shelf (Lambeck, 1996) and >800 m thick along the Svalbard west coast (Lambeck, 1995). The ice front retreated rapidly, as the shelf west of Svalbard was deglaciated by *c.* 15 ka BP (Landvik *et al.*, 1998), and the middle part of Isfjorden (Fig. 1A) was ice-free by 10·5 ka (Elverhøi *et al.*, 1995; Svendsen *et al.*, 1996). The ice front here receded along the main fjord and its inland branches, while retreating also from the adjacent mountain plateaux and leaving behind isolated glaciers. The inner Isfjorden, its head branches and at least some of the coastal catchments were ice-free by 10 ka BP (Svendsen & Mangerud, 1992, 1997). The Adventfjorden (Fig. 1A), Isfjorden's south-eastern tributary, was deglaciated at this time, when the Hiorthfjellet fan delta began to form on its north-eastern coast (Fig. 1B) and a fjord-wide braidplain delta started to prograde from the fjord head zone. The sedimentation history of the fjord-side Hiorthfjellet fan delta is the focus of the present study. The U-shaped fjord here was *c.* 80 m deep, covered with glaciomarine deposits up to 10–12 m in thickness (Elverhøi *et al.*, 1995). The Adventdalen braidplain delta has prograded by *c.* 10 km along the fjord (Johansen *et al.*, 2003), and its toe is presently encroaching upon the subaqueous part of the Hiorthfjellet fan delta (Fig. 1A).

Many of the isolated relic glaciers, particularly on south-facing slopes, had gradually melted, whereas others survived until the onset of the Neoglacial stage 4–5 ka BP and even increased in size until the Little Ice Age, which had its maximum here in the late nineteenth century. At present, nearly 60% of the Svalbard area remains glaciated.

The relative sea level has fallen as a result of post-glacial crustal rebound, which markedly exceeded the coeval glacioeustatic sea-level rise. The shoreline displacement curve from the Kapp Ekholm area in east-central Spitsbergen (Salvigsen, 1984) indicates a marine limit (i.e. the highest relative sea-level stand) at present-day altitude of 90 m and a relative sea-level fall to its recent position at a declining rate. The marine limit in outer Adventfjorden is at an altitude of *c.* 70 m (Fig. 1A) and decreases to 62 m approximately 16 km to the south-east in Adventdalen, where a raised beach has been dated to *c.* 10 ka (sample T-13882 in Table 1).

The polar desert climate

Svalbard has a permafrost layer 100–450 m thick (Liestøl, 1976), with an active (seasonally melting) surficial layer of 0·5–1 m. The annual precipitation is very low, averaging 190 mm, and most of it is snow. The air temperature varies between a February mean of −15·2 °C and a July mean of 5·9 °C, averaging −6·7 °C (data from Svalbard airport in outer Adventfjorden; Førland *et al.*, 1997). The surficial runoff of meltwater is limited to two or three summer months, when it is accompanied by sparse rainfall (Gjessing *et al.*, 1990). The winter season spans 9–10 months, when Advantfjorden freezes over for 6 months on average. The local tidal range is around 1 m. The tides drive under-ice water circulation and often break the ice cover along the shore, piling ice slabs onto the beach.

Winds persistently sweep the high-relief landscape of fjords, valleys and rolling plateaux, causing ubiquitous snow drift, particularly in valleys trending approximately east–west, such as Adventdalen (Fig. 1A). On average, the Adventfjorden area has 5–14 days a month with winds stronger than 14 m s^{-1} and up to 5 days with winds exceeding 25 m s^{-1} (Førland *et al.*, 1997). The strongest winds predominate in winter. Snowpack thicker than 1 m accumulates only in local wind shadows, mainly as cornices on lee slopes and in ravines and stream channels. In the study area, the fan-delta surface is covered with thin ice throughout winter, and the snow cover here reaches 1 m or more only in the fan delta's low-lying active sector, head channel and adjacent mountain slope ravines.

The strong winds and sparse vegetation render evaporation very high, with a considerable amount of snow and ice vanishing by direct atmospheric sublimation. Nevertheless, the air is dry, even by comparison with many hot arid regions. The water-vapour capacity of cold air is very low, averaging *c.* 1 g of vapour per kg of air in winter and little more than 5 g kg^{-1} in the

Table 1. Radiocarbon dates from the Hiorthfjellet fan delta and two adjacent localities in Adventfjorden and Adventdalen.

Laboratory sample code	Locality	Material dated	^{14}C age	Calibrated age BC	Escarpment section's distance point (m)	Relative distance in foreset dip direction (m)	Facies assemblage
T-13882	Bolterdalen	*Mya truncata*	10025 ± 160	–			Raised beach, altitude 62 m
T-11575	Blomsterdalen	*Mya truncata*	9940 ± 115	–			Marine mud, altitude 50 m
T-13345	Hiorthfjellet	*Mytilus edulis*	6175 ± 90	5200–4955	215	0	Proximal fan-delta foreset
T-13346	Hiorthfjellet	*Mytilus edulis*	6090 ± 120	5130–4830	245	27	Medial fan-delta foreset
T-13347	Hiorthfjellet	*Mytilus edulis*	6235 ± 85	5235–5040	255	36	
T-13348	Hiorthfjellet	*Mytilus edulis*	6260 ± 135	5280–5010	265	45	
T-13349	Hiorthfjellet	*Mytilus edulis*	6190 ± 90	5210–4970	275	54	
T-13350	Hiorthfjellet	*Mytilus edulis*	5905 ± 50	4825–4715	290	67·5	Distal fan-delta foreset
T-13351	Hiorthfjellet	*Mytilus edulis*	5820 ± 70	4760–4575	310	85·5	
T-13352	Hiorthfjellet	*Mytilus edulis*	5620 ± 95	4540–4340	325	99	
T-13353	Hiorthfjellet	*Mytilus edulis*	5575 ± 50	4330–4145	340	112·5	
T-13354	Hiorthfjellet	*Mytilus edulis*	5495 ± 65	4370–4250	365	135	
T-13355	Hiorthfjellet	*Mytilus edulis*	5155 ± 135	4090–3790	385	153·4	Distal-most fan-delta foreset
T-13356	Hiorthfjellet	*Mytilus edulis*	4965 ± 65	3795–3665	405	171·8	and terminal beach
T-13357	Hiorthfjellet	*Mytilus edulis*	5045 ± 115	3960–3690	435	199·4	
T-13358	Hiorthfjellet	*Mytilus edulis*	4350 ± 110	3120–2870	470	231·6	Post-spit regressive beach

The data from the fan-delta escarpment section are listed according to their horizontal seaward distance (cf. Figs 3 and 4); these apparent distances are also recalculated into the true relative distances in the direction of delta-front progradation.

summer, while only around 73% of this capacity is saturated (Førland *et al.*, 1997).

Geomorphic processes

The high-relief landscape of Svalbard, sculptured by successive Pleistocene ice sheets, has been subject to intense gravitational wastage during interglacial periods, when the fjords and valleys were lined with sediment. The Holocene geomorphic processes include local proglacial outwash, fluvial modification of glacial valleys, progradation of fjord-head deltas and considerable slope wasting (Jahn, 1967; Lægreid, 1999; Soltvedt, 2000). The principal source of flowing water is the summer melting of snow, glaciers and the active layer, combined with rain showers (Gjessing *et al.*, 1990). Bedrock weathering is driven chiefly by frost, and rockfalls abound on the barren cliffs of fractured sedimentary rocks. The debris masses accumulating in slope ravines act as sieves, entrapping successively finer particles, growing in volume and becoming metastable. Massflow avalanches occur when the debris mass in a ravine or the melted active layer on a steep slope is destabilized, typically by a spell of extreme weather conditions, such as air temperature peak or heavy rainfall (Larsson, 1982). Localized accumulation of snowdrift on high slopes occasionally leads to a snowflow avalanche, or a slushflow triggered by rain (Jahn, 1967). All these slope-wasting phenomena are referred to jointly as colluvial processes (Blikra & Nemec, 1998).

Bedrock geology

The bedrock exposed on the northern side of Adventfjorden (Fig. 1B) is a layer-cake succession of Early Cretaceous and Palaeocene siliciclastic rocks, inclined slightly to the south-west (Fig. 2, profile A; Major *et al.*, 2000). The lowest mountain slope consists of the uppermost Rurikfjellet Fm. (*c.* 70 m thick), composed of dark-grey shales with thin siltstone and sandstone sheets. The cliff-forming Helvetiafjellet Fm. above consists of light-grey sandstones (*c.* 50 m) overlain by darker sandstones interbedded with siltstones, shales and minor coal seams (*c.* 100 m). The overlying Carolinefjellet Fm. (*c.* 200 m) comprises shales alternating with sandstone sheets, the former predominant in the middle part. The erosional base of the overlying Palaeocene rocks is a subtle angular unconformity. The Firkanten Fm. (*c.* 210 m) consists of grey sandstones, siltstones, shales and coal beds in its lower part and whitish-grey sandstones in the upper part. The Basilika Fm. (*c.* 90 m) consists of shales intercalated with siltstone and minor sandstone beds. The cliff-forming Grumantbyen Fm. at the top is composed of greenish-grey sandstones (*c.* 150 m). The apical part of Hiorthfjellet consists of shales, a relic basal portion of the younger Frysjaodden Fm. (Dallman *et al.*, 2001).

The high-relief bedrock slope is prone to physical weathering and denudation, shedding an immature mixture of angular gravel, up to boulder in size, and second-cycle sand and mud. The clasts of sandstone and siltstone are mainly platy or cubic to rhomboidal in shape.

The catchment and fan morphology

The Hiorthfjellet fan delta is a radial accumulation of coarse sediment at the coastal foot of Hiorthfjellet mountain ridge in Adventfjorden (Fig. 1). The fan apex is at an altitude of *c.* 85 m, and the south-facing high-relief catchment extends to the mountain top at 923 m (Fig. 1B). The catchment has a plan-view area of 2·6 km^2 and consists of two slope recesses (Fig. 1B): one with a system of coalescing V-shaped ravines (sector I) and the other with the scoop-shaped morphology of a glacial cirque (sector II), both modified by flowing water and colluvial processes. The slope gradient in each sector varies, which renders their longitudinal profiles segmented (see slope segments *a*–*d* in Fig. 1B). Little sediment has accumulated in slope segment I*a*, whereas segment II*a* has a cover of glacial and talus debris and an active rockglacier in the lower part (Fig. 1B). The slope gradient here decreases from 0·82 to 0·45 (Fig. 2, profile A). The narrow lower segments I*b* and II*b* (Fig. 1B), with V-shaped transverse profiles and an axial gradient of *c.* 0·27, have been scoured by flowing water and contain more debris. They converge downslope into a short V-shaped passage (segment *c* in Fig. 1B), richer in debris, leading to the depositional fan delta proper below (segment *d* in Fig. 1B).

The larger of the two recesses, with the cirque morphology, indicates that the mountain slope here was subject to localized subglacial erosion down to an altitude of 350 m and thus must have hosted a temperate glacier for some time after the fjord deglaciation. The shallow U-shaped depression at the crest of Hiorthfjellet, above the cirque (Fig. 1B), suggests that the thick glacier in the adjacent valley, Mälardalen, probably spilt over

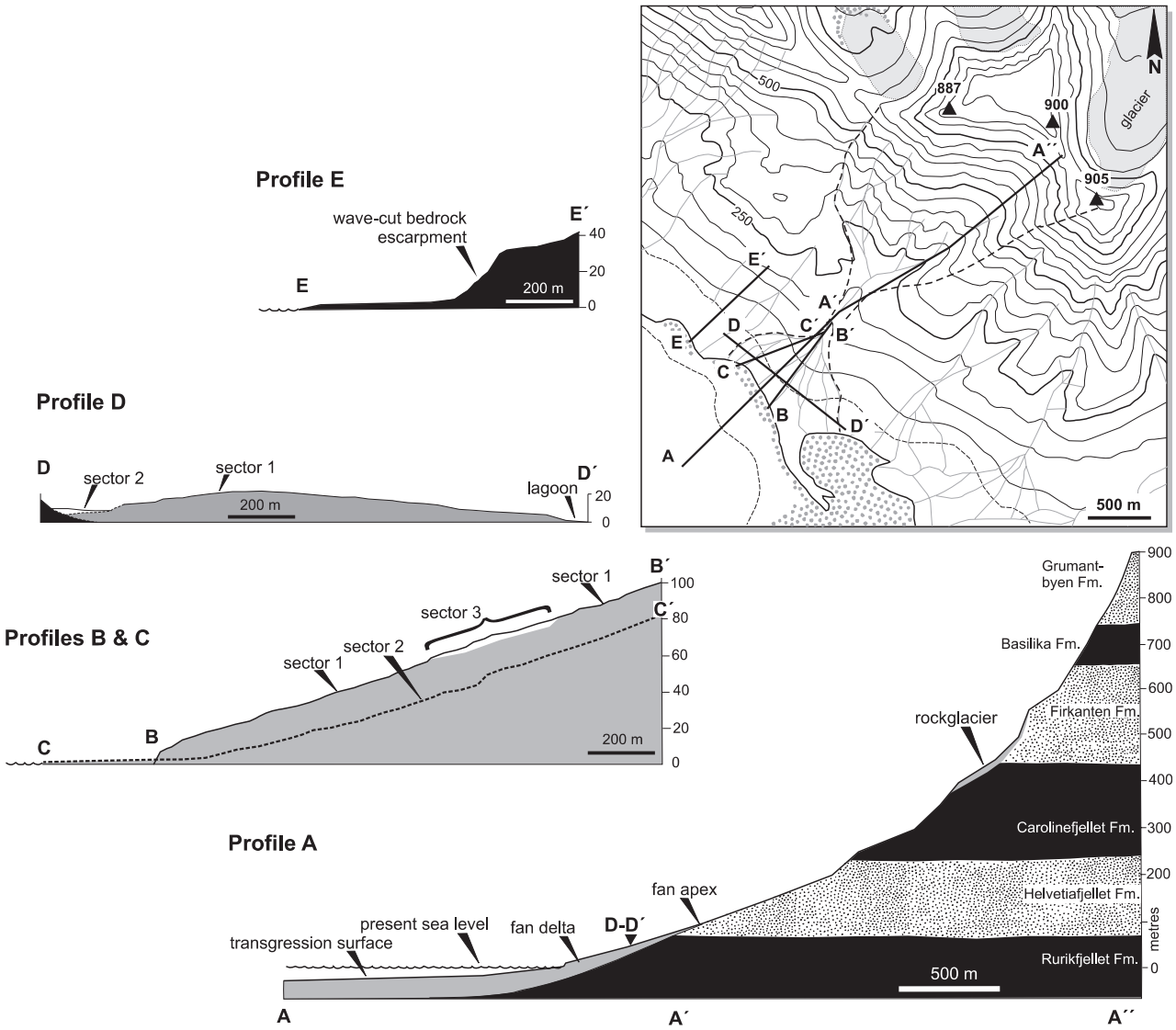

Fig. 2. Topographic map of the Hiorthfjellet area (inset), showing the location of morphometric profiles A–E. Profile A is based on a 1:100 000 scale topographic map (Major *et al.*, 2000), and the other profiles are based on an unpublished 1:10 000 scale map (Svalbard Samfunnsdrift). Note the bedrock formations indicated in profile A.

the mountain crest, adding ice to this isolated cirque glacier. The cirque glacier and possibly other ice remnants in the catchment are thought to have supplied flowing water that deposited the main part of the Hiorthfjellet fan delta. The catchment today yields relatively little water, and the main supply of sediment is by colluvial processes. The smooth transition from the cirque segment II*a* to the water-scoured segment II*b*, mantled with fresh debris, testifies to an active sediment supply.

The alluvial fan has a convex-upward transverse profile (Fig. 2, profile D), whereas its axial profile is raised and nearly planar, with a gradient of 0·11 (Fig. 2, profile B), apparently graded to a higher relative sea level. The longitudinal profile of the fan active sector (Fig. 2, profile C) is considerably lower, incised and slightly concave upwards, with a gradient decreasing from 0·13 to 0·06 and flattening out at the shore. The bedrock coast lateral to the fan delta shows a wave-cut escarpment at an altitude of around 10 m (Figs 1B and 2, profile E).

Anthropogenic activity

The study area, like most of the Svalbard region, has been little affected by human activity. A small mine operated in the Hiorthfjellet catchment for a few years between 1917 and 1940, digging coal

from the lower part of the Firkanten Formation (Fig. 2, profile A) and using a cableway linking the mine entrance at 450 m altitude (in slope sector I*a*, Fig. 1B) with a docking facility on the shore (Dallman *et al.*, 2001). The total amount of coal derived from the mine is estimated at *c.* 100 000 tonnes, but the mining involved a thick coal seam, was manual and produced little waste, and its impact on the local landscape and modern sediment yield was minimal. Some traces of that activity, such as tin cans and wooden planks, are found scattered on the fan surface by modern snow avalanches.

THE HIORTHFJELLET FAN DELTA

For the purpose of the ensuing chronological description of the deposits and processes, the fan delta has been divided into three sectors (Figs 1B and 3A). Sector 1 corresponds to the original fan delta at its maximum lateral extent, with the topset alluvium and the upper part of subaqueous foreset unit well exposed. More than 70% of the fan delta's terrestrial surface is presently inactive and thinly covered by tundra vegetation (mainly *Cassiope* and *Dryas* heath). Sector 2 is the incised active part of the fan, which is divided further into three subsectors (labelled 2a–c in Fig. 3A) on the basis of its morphology and inferred chronology of fluvial activity. Sector 3 is a narrow zone on the inactive fan surface, near the apex, where debris supplied by modern snow avalanches has accumulated.

Sedimentation in sector 1

This sector has an angular width of 110° (Fig. 3A), and its deposits, chiefly gravel and sand, constitute the bulk of the fan delta. Its distal part has been shallowly eroded by waves and is submerged (see offshore bathymetry in Fig. 3A). The deposits have been studied in a shoreline escarpment section oblique to the fan radius (Fig. 3B), extending from the proximal/medial transition to the distal part of the fan delta. The outcrop section (Fig. 4) shows a foreset of steeply inclined, seaward-accreted fossiliferous subaqueous deposits overlain by a topset of flat-lying alluvium, up to 4 m thick, suggesting a Gilbert-type fan delta. Only the upper part (up to 6 m thick) of the fan-delta foreset is exposed, but the foreset unit here may be at least 10 m thick and is estimated to have reached a thickness of possibly up to 25 m at the offshore outer perimeter of the fan delta (see the maximum extent in Fig. 3A).

The component facies assemblages of the fan delta have been mapped in the outcrop section to establish their spatial and stratigraphic relationships, with the aid of radiocarbon dates from shells. A conventional ^{14}C-dating method was used and the results are listed in Table 1 (for sample locations, see Figs 3B and 4). The spatial relationships observed are an integral part of the ensuing facies analysis and, hence, are first summarized as a guide to the spectrum of facies assemblages that are subsequently described and interpreted.

The alluvial topset has an uneven, erosional base and is separated from the foreset by a unit of delta-front beach gravel in the medial to distal part of the fan delta (Fig. 4). The alluvium pinches out seawards, *c.* 920 m away from the fan apex, but the accretionary foreset persists over a considerable distance (Fig. 4), *c.* 160 m in the dip direction. The altitude of the delta-front beach ridge decreases seawards, and the most distal part of the outcrop section shows aggradational beach deposits (> 2 m thick) overlain by the landward-accreted foreset of a transgressive gravelly spit (Fig. 4, bottom). These spit platform deposits, up to 1·5 m in thickness, have onlapped the fan-delta plain to an altitude of *c.* 6 m, slightly overstepping the pinchout point of the topset alluvium (Fig. 4, top right). The youngest deposits in the outcrop section are the shallow fluvial palaeochannels scattered along its top and the seaward-accreted, regressive, fossiliferous beach deposits at its distal end (Figs 3B and 4, bottom right), both clearly post-dating the transgressive spit platform.

Fan-delta foreset facies

The fan-delta foreset consists of alternating sand and gravel beds, with minor intercalations of mud and silt. The beds are inclined at 25–30° and are gently convex upwards, but planar in a downdip direction. In the medial to distal part of the fan delta (outcrop distance 215–425 m in Fig. 4), the steep foreset beds interfinger with the low-angle to subhorizontal strata of an overlying, coeval gravelly unit interpreted as the delta-front beach deposits (Fig. 5A and B). In the proximal part, this latter facies is lacking, and the foreset deposits are erosionally overlain directly by alluvium (Fig. 4, top left). The component facies and depositional architecture of the fan-delta foreset unit are described and interpreted below, based on detailed logs from

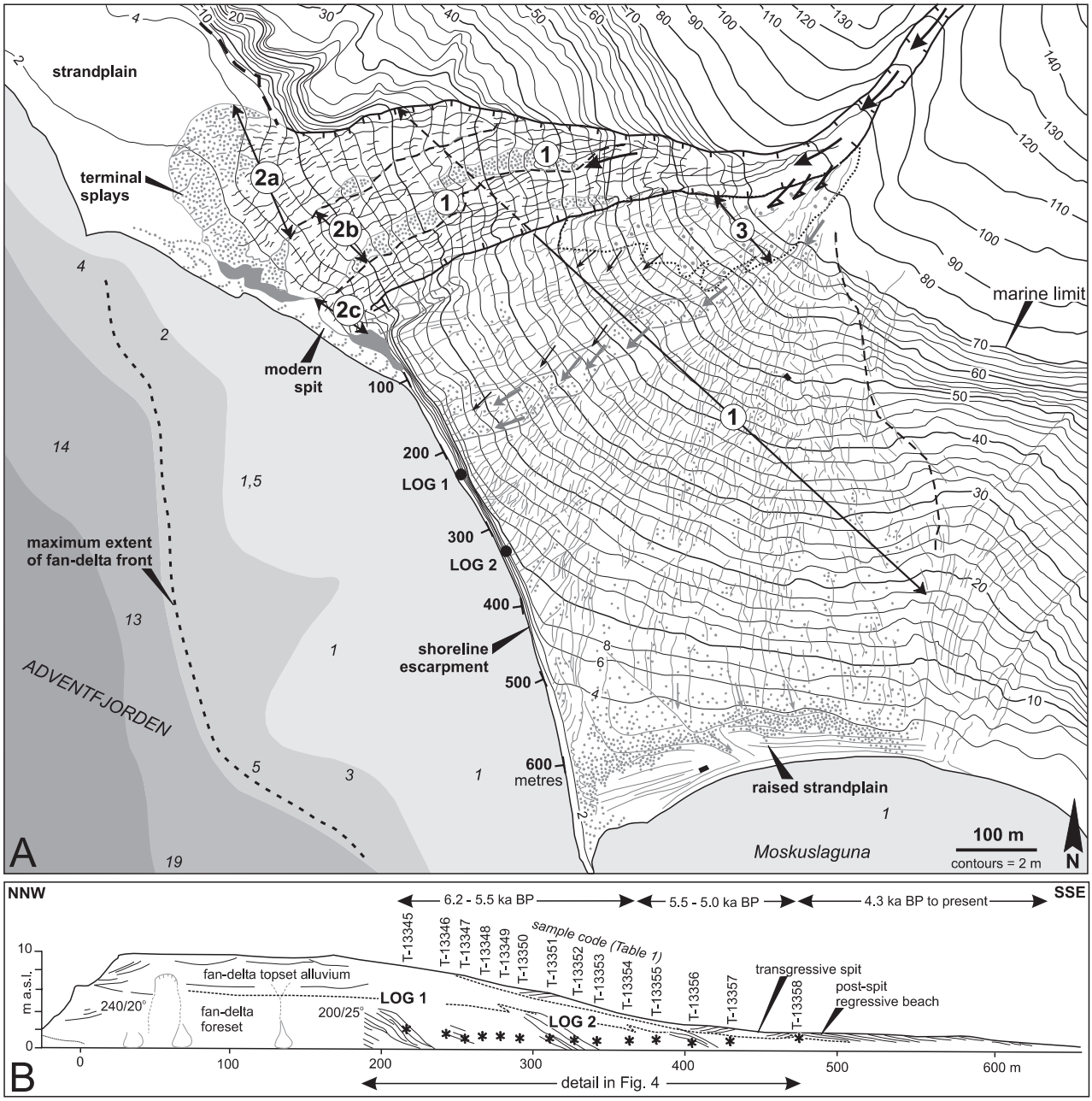

Fig. 3. (A) Detailed morphology of the Hiorthfjellet fan delta, shown as a combination of the fjord bathymetric map, a subaerial topographic map at 1:10 000 scale (Svalbard Samfunnsdrift) and an overlay drawing from a 1990 infrared aerial photograph at 1:15 000 scale (Norwegian Polar Institute, S90-5402). The morphological lineaments drawn are relic fluvial features, modern accretionary spits and raised strandplain ridges. The maximum seaward extent of the fan delta is hypothetical, based on the fjord bathymetry and delta-plain morphology. The fan sectors are as defined in Fig. 1B. The active sector 2, divided into three subsectors, contains relic terraces of the original alluvium of sector 1 (dotted). Note the modern shoreline escarpment and the location of logs 1 and 2. (B) Simplified sketch of the shoreline escarpment section (vertical scale exaggerated), showing the distribution of main facies assemblages and the location of radiocarbon-dated samples (Table 1) and logs 1 and 2.

the proximal/medial and distal parts of the outcrop section (Figs 6 and 7; see log locations in Fig. 4). In the description, the orientation of gravel clasts is defined relative to the foreset dip direction.

Massflow sand. These are massive beds of fine to very coarse sand, generally well sorted, but commonly texturally inverted (*sensu* Folk, 1974). For example, many beds consist of a mixture of fine and very coarse sand, or of fine to medium sand rich in

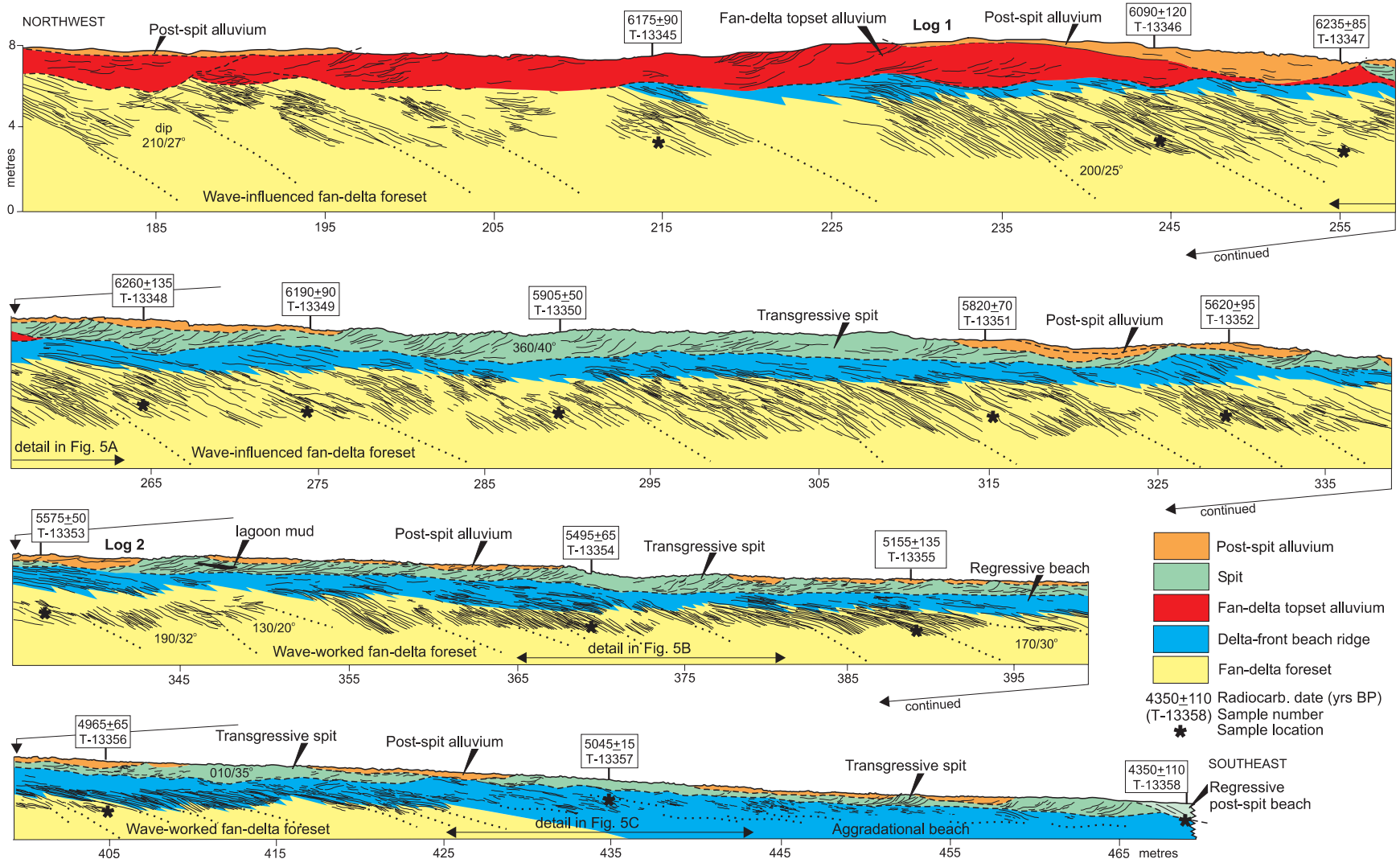

Fig. 4. Overlay drawing from a photomosaic of a large part of the shoreline escarpment section indicated in Fig. 3 (central segment, distance interval from 176 to 470 m), showing the depositional architecture of the fan delta in sector 1. In the text, the left-hand half of the upper panel is referred to as the 'proximal' and the lower two panels as the 'distal' part of the fan delta; the intermediate segment of the section is referred to as the 'medial' part. The solid lines are traces of bedding surfaces and gravel clast alignments, whereas the colours indicate the main facies assemblages (see legend). Note the locations of the radiocarbon-dated samples (Table 1), logs 1 and 2 (Figs 6 and 7) and the detailed panels shown in Fig. 5.

granules and occasionally also in mud. Beds are 1–32 cm thick, averaging 4 cm. They commonly contain scattered granules and/or floating blade-shaped pebbles with dip-aligned long axes, and some also bear spherical cobbles. The beds generally lack grain-size grading, except for a few thin beds that show inverse grading. The deposits are attributed to non-turbulent sandflows with plastic rheology (debrisflows), ranging from cohesive to cohesionless and including thin grainflows. These subaqueous massflows are thought to have been generated by gravitational collapse of the wave-worked front of the fan delta, when undercut by storm waves or destabilized by stream floods (Nemec *et al.*, 1999; Lønne *et al.*, 2001). The thin grainflows were probably caused by backwash (Sallenger, 1979). This facies constitutes 47 vol.% of the delta foreset unit in the proximal log 1 (Fig. 6) and only 16 vol.% in the distal log 2 (Fig. 7).

Massflow gravel. These are massive beds of granule gravel (2–5 cm thick) or pebble gravel (mainly 10–40 cm thick), with a sand matrix and clast- to matrix-supported texture. Clasts are mainly subrounded to rounded, and the gravel varies from moderately to well sorted, commonly within a single bed (Fig. 8F). Some beds bear floating outsized cobbles, with dip-aligned long axes, either parallel to the foreset bedding or updip inclined. Many beds show crude inverse or inverse-to-normal grading and a steepening-upward or sigmoidal, steepening- to flattening-upward clast fabric (Fig. 8F). Similar fabrics have been described from gravelly massflow deposits on steep beachfaces (Massari & Parea, 1988; Massari, 1996) and delta slopes (Nemec, 1990; Nemec *et al.*, 1999). The gravel beds are commonly lenticular and slightly erosional, thicker in their downdip part and thinning updip (Fig. 8A), as is typical of many plastic massflows that 'freeze' on steep slopes (Blikra & Nemec, 1998; Nemec *et al.*, 1999). These gravelly deposits are attributed to cohesionless debrisflows generated by gravitational collapse of the delta-front beach ridge, when undercut by storm waves or swept by stream floods. This facies constitutes 10 vol.% of the fan-delta foreset unit in the proximal log 1 (Fig. 6) and 6·5 vol.% in the distal log 2 (Fig. 7).

Wave-worked sand and gravel. These are units of stratified sand, gravelly sand and gravel, mainly 5–50 cm thick, showing rapid vertical and lateral grain-size changes (Fig. 8A and G). Sand is well sorted, but varies from fine to very coarse in alternating layers, which commonly contain scattered pebbles or abundant granules and are intercalated with layers of granule or fine pebble gravel. Gravel clasts are aligned mainly parallel to the foreset strike, with a bedding-parallel or updip-inclined fabric (Fig. 8D and G). Fine sand units commonly show wave-ripple cross-lamination (Fig. 8D and E), mainly asymmetrical, dipping upslope, whereas the coarser sand and gravel are plane-parallel stratified (Fig. 8D and G). Units of alternating sand and gravel are separated by nearly planar erosional surfaces, recognizable as subtle to distinct angular unconformities with toplap, downlap or onlap stratal patterns (Fig. 8C and D). Similar deposits characterize foreshore zones (Komar, 1976; Massari & Parea, 1988), and this facies is thought to have been deposited by wave traction on the delta's upper subaqueous slope acting as a reflective beachface (cf. Lønne *et al.*, 2001). The cross-laminated sand indicates preferential shoreward transport by swash during periods of low wave energy, whereas the planar stratification and shoreward-imbricated pebbles in coarser layers indicate prevalent seaward transport by backwash during periods of higher wave energy. The internal truncations indicate erosion by storm waves. Planar stratification is far more abundant than ripple cross-lamination, which reflects the low preservation potential of fairweather deposits on a reflective beachface (Komar, 1976; Massari & Parea, 1988; Briseid, 1994). The scattered outsized cobbles and large pebbles, mainly spherical and isolated or clustered (Fig. 8A–C), resemble the outer frame deposits of a beachface toe (Bluck, 1999). They are more common in the distal part of the fan delta (Fig. 7). The runout of large mobile clasts on the steep delta slope was considerably enhanced by gravity, and their downslope emplacement as an extended outer frame facies is attributed to debrisfall processes (*sensu* Nemec, 1990), instigated by storm backwash. The wave-worked deposits constitute 18 vol.% of the fan-delta foreset unit in the proximal log 1 (Fig. 6), but as much as 48 vol.% in the distal log 2 (Fig. 7).

Hemipelagic mud and associated tidal deposits. Mud layers, mainly thinner than 5 cm and isolated, occur repeatedly throughout the fan-delta foreset section (Figs 6 and 7). The dark-grey mud shows black horizons rich in seaweed detritus and also contains light-grey silty bands and discrete interlayers of cross-laminated silt or very fine sand. The ripple cross-laminated

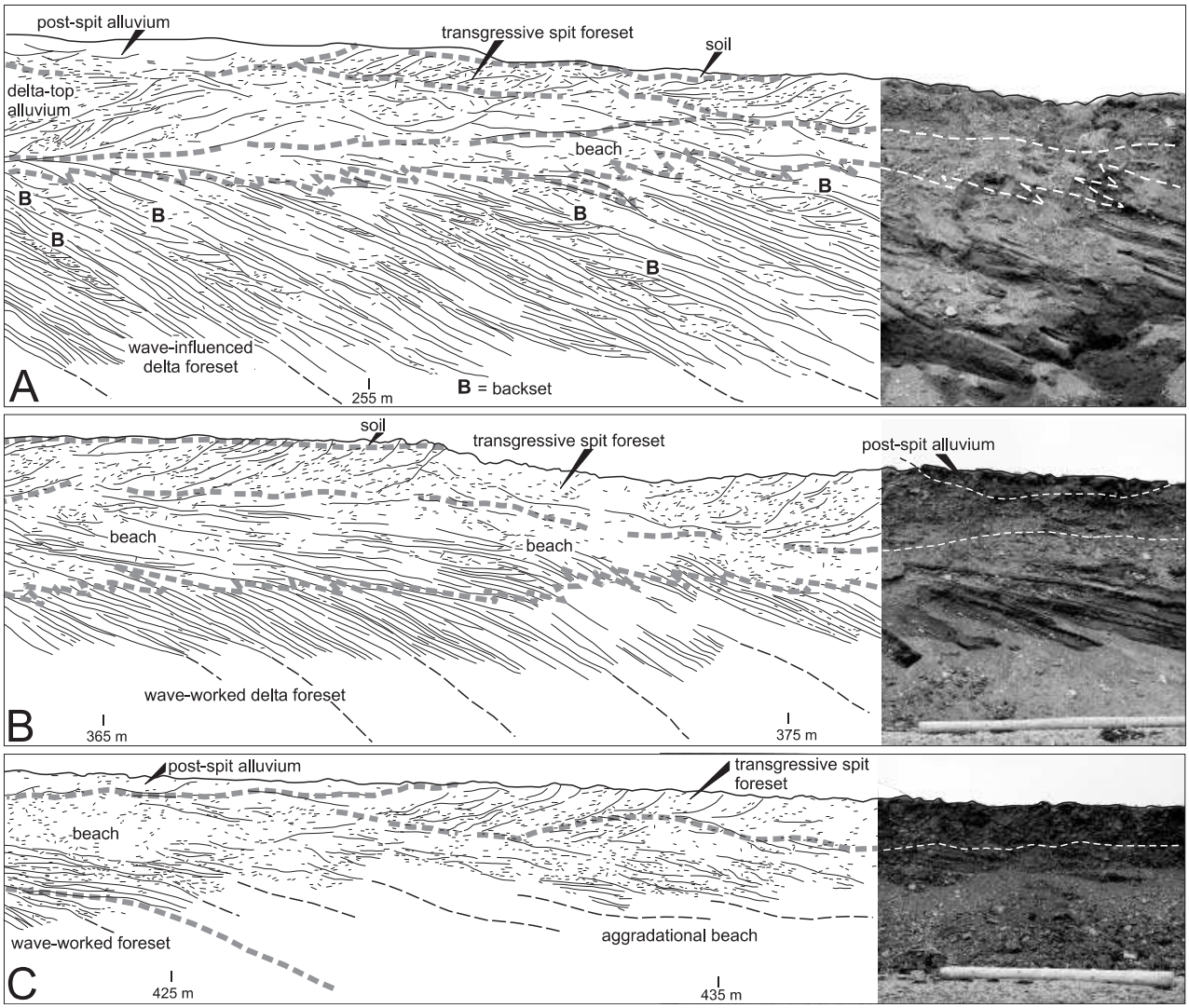

Fig. 5. Close-up details of the outcrop section shown in Fig. 4 (see reference distances), showing the bedding geometry and stratigraphic relationship of the main facies assemblages; overlay drawings from outcrop photomosaic combined with closer photographs. (A) The fan-delta foreset and alluvial topset separated by delta-front beach facies, overlain by transgressive spit deposits and a post-spit fluvial palaeochannel; note the numerous internal unconformities and isolated backsets (*B*) in the delta foreset unit. (B) The more distal, wave-worked foreset and associated beach-ridge facies of the fan delta, overlain by transgressive spit deposits, post-spit fluvial palaeochannel and soil; note the smooth, convex-upward transition from the foreset to beach strata and the lack of alluvial topset. (C) The distalmost wave-worked foreset and beach facies, passing seawards into aggradational beach deposits and overlain by the transgressive spit unit and younger fluvial deposits.

layers show mud flasers, are commonly developed as horizons of poorly interconnected lenses (starved ripples) and generally indicate deposition by weak seaward currents. Redeposited seaweeds, in the form of paper-thin lenses (patches) and broader laminae (mats), are common at the boundaries of these layers (Figs 6, 7 and 8F). The repetitive occurrence of this quiet-water heterolithic facies within the wave-dominated delta-face succession indicates periodic cessation of wave activity, which suggests deposition in winter, when the fjord was covered with ice. The interlayers of silt and sand are attributed to tidal ebb currents, whereas the dead seaweeds may have been dragged into the foreshore zone by tidal floods. The fine-grained deposits of the fjord's winter slackening phase would generally be eroded by subsequent wave action and, hence, the muddy units in the delta foreset succession are probably little more than a record preserved by chance. This facies constitutes only 7 vol.% of the fan-delta foreset unit in the proximal log 1 (Fig. 6) and 16·5 vol.% in the distal log 2 (Fig. 7).

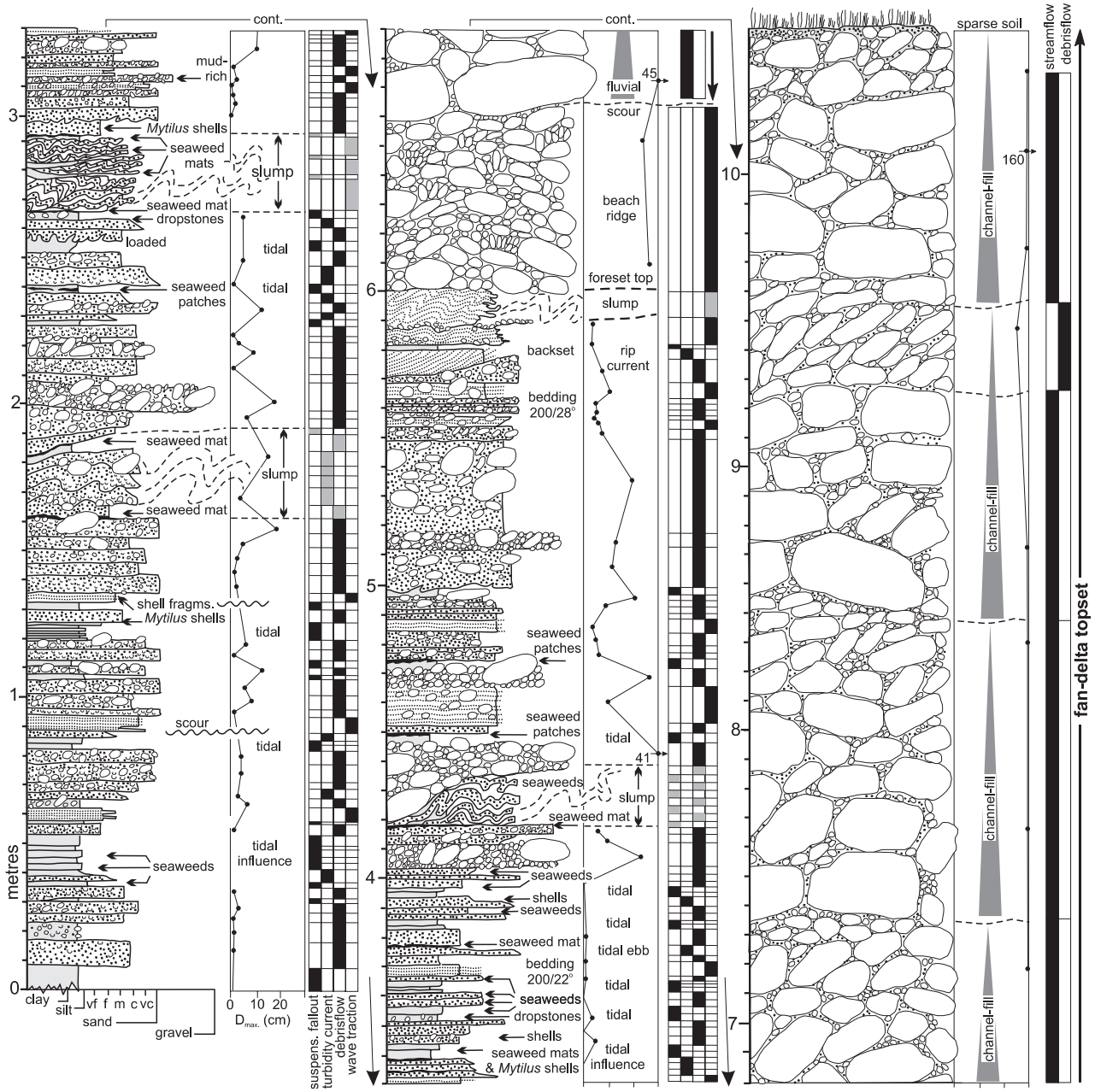

Fig. 6. Sedimentological log 1 from the transitional proximal/medial part of the fan-delta section (see location in Fig. 4, top), showing the strongly wave-influenced delta foreset, frontal beach deposits and topset alluvium. The log is normal to the foreset bedding and corresponds to a horizontal distance of *c.* 16 m; foreset bed inclination not shown.

Turbidites. The fan-delta foreset also contains thin beds of massive sand, mainly 2–6 cm thick, that show distinct normal grading in a grain-size range of very coarse to fine sand, medium/fine to very fine sand or fine sand to silt (Figs 6 and 7). These beds are mainly isolated, but occasionally two or three are stacked directly upon one another (e.g. see log interval 3·3–3·4 m in Fig. 6). The thinner, finer grained beds are associated with the muddy, tide-influenced facies and the coarser ones with the wave-worked facies. The normal grading and lack of stratification indicate rapid, non-tractional deposition from turbulent suspension, which suggests high-density turbidity currents (Lowe, 1982). Given the small thickness, varied grain size, inconsistent facies association and non-tractional mode of deposition of these beds, the turbidity currents must have been brief surges, volumetrically small and poorly ignited. These deposits differ markedly

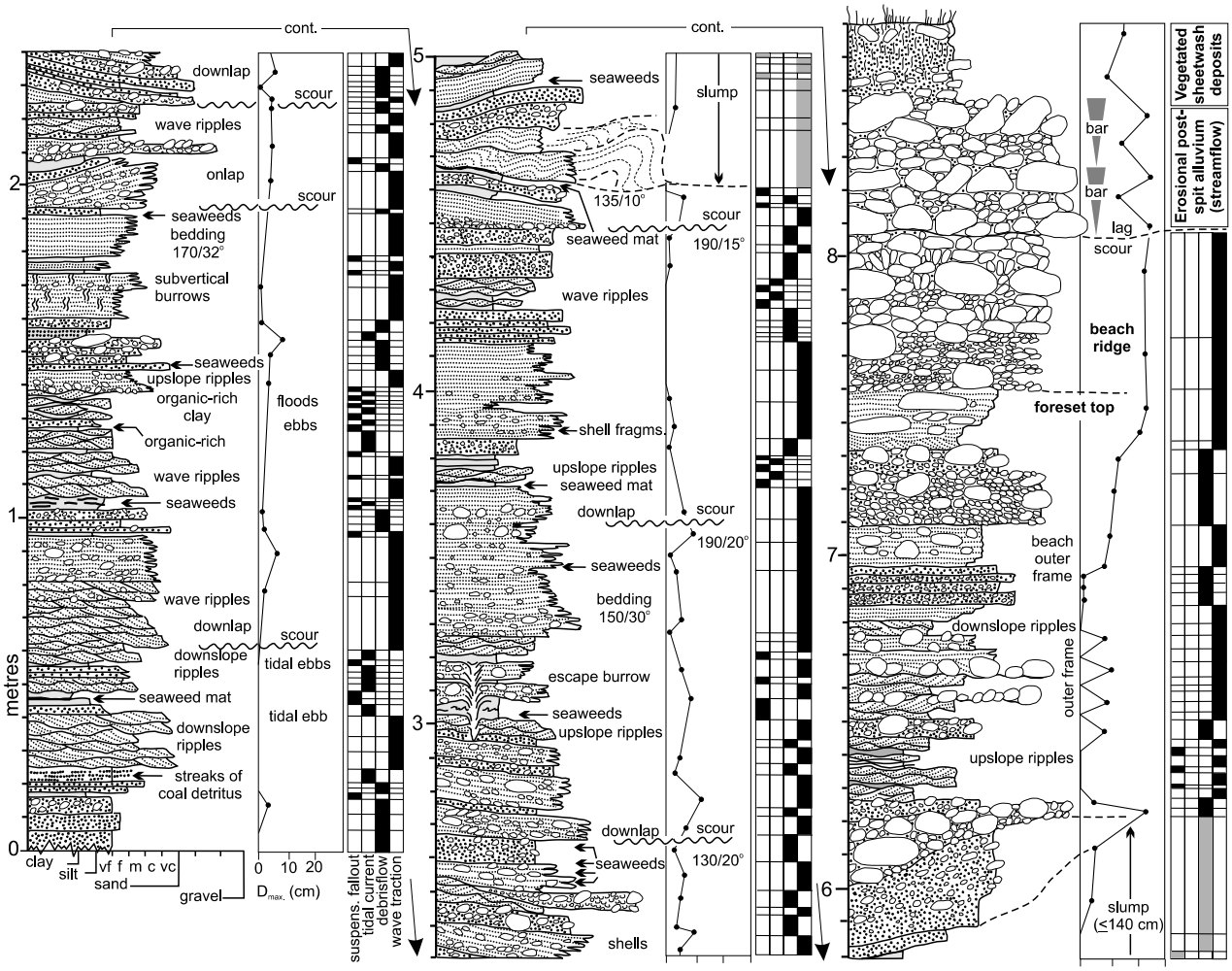

Fig. 7. Sedimentological log 2 from the distal part of the fan-delta section (see location in the lower-middle part of Fig. 4), showing the wave-worked foreset and frontal beach deposits overlain by a younger, post-transgression alluvium. The log is normal to the foreset bedding and corresponds to a horizontal distance of *c.* 19 m; foreset bed inclination not shown.

from the thick packages of amalgamated sandy to gravelly turbidites that abound in glacial Gilbert-type deltas at mid-latitudes (Postma & Cruickshank, 1988; Nemec *et al.*, 1999; Lønne *et al.*, 2001), and the discrete, infrequent surges are unlikely to have been hyperpycnal underflows caused by stream floods. The delta front lacks mouth bars and cross-cutting chutes, which indicates that the stream effluent was incapable of spreading much fluvial sediment beyond the beach zone or generating robust hyperpycnal currents. The extremely cold and wave-agitated fjord waters would be likely to render the effluent homopycnal to hypopycnal (Nemec, 1995). The small turbidity currents are thus inferred to have been generated by the spring-phase tidal drawdown (cf. Smith *et al.*, 1990) in winter, when the fjord was frozen over, and by the storm-generated backsurges of sand-laden water (Komar, 1976; Massari & Parea, 1988; Massari, 1996). This interpretation is consistent with the varied facies association of these turbidites in the fan-delta foreset unit (Fig. 6). The preservation potential of such deposits on a wave-dominated delta slope would be very low, and hence this facies is volumetrically negligible, constituting little more than 1 vol.% of the proximal log 1 (Fig. 6) and practically lacking in the distal log 2 (Fig. 7).

Slump deposits. Some of the foreset beds are internally deformed, showing asymmetrical or recumbent hydroplastic folds overturned in a downdip direction (Figs 6 and 7), discrete, updip-inclined shear bands or small thrusts (Fig. 8F) and sharp basal detachment surfaces, commonly lined with seaweeds and truncating

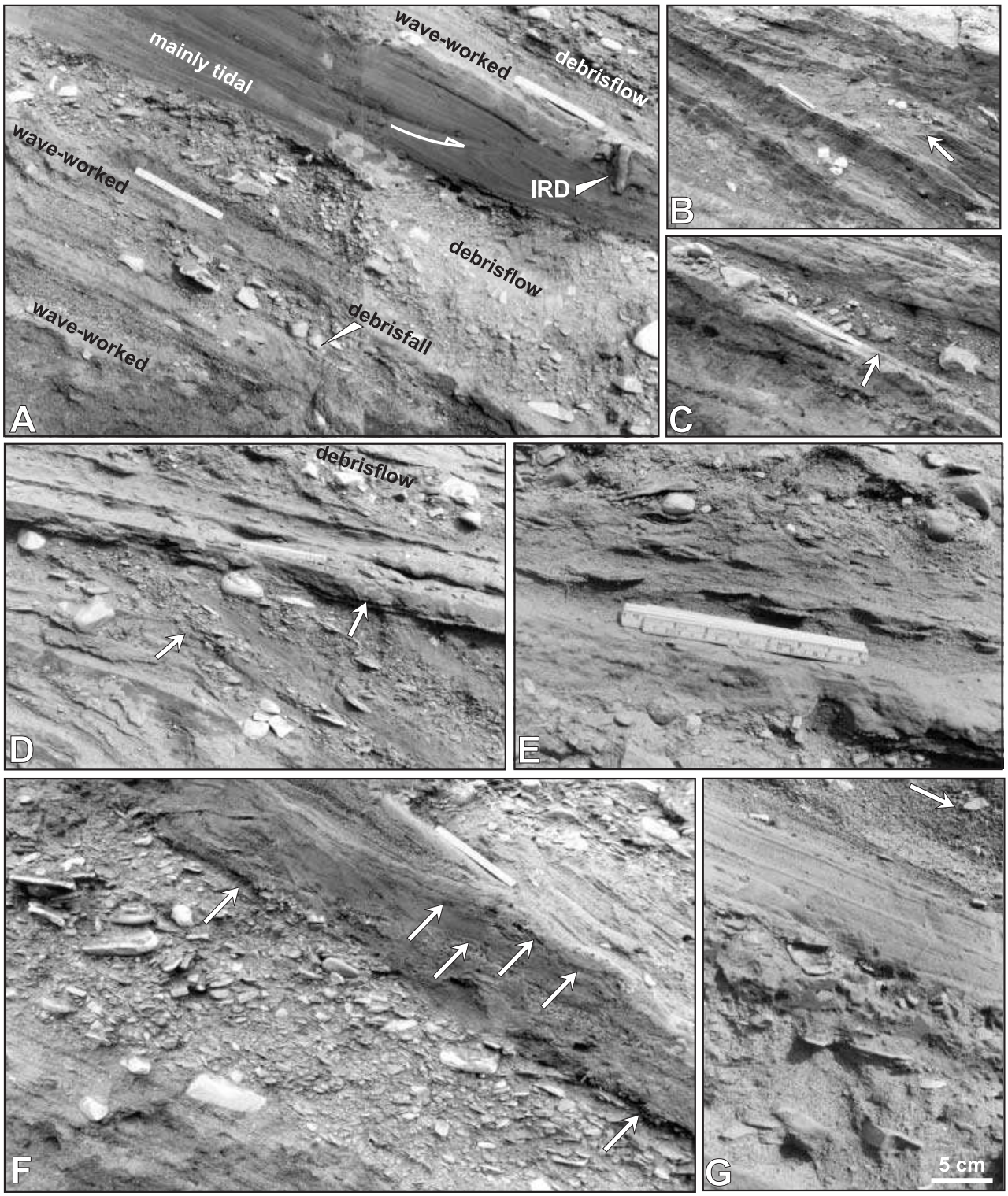

the substrate slightly (Fig. 8A and F). These units are mainly 20–30 cm thick, but their mounded downslope parts are occasionally up to 140 cm in thickness. The sediment is recognizably a deformed and displaced slab of one or more of the other foreset facies, typically including the muddy heterolithic deposits (Fig. 8F). These deformed units are apparently slump deposits, as is indicated also by listric, scoop-shaped slump scars (Fig. 9A, top) and truncated relics of deformed *in situ* strata (Fig. 8A) within the foreset succession. The slumping of delta-slope

Fig. 8. Fan-delta foreset facies (details from outcrop section in Fig. 4); the foreset dip direction is obliquely to the right, at *c.* 30–45° out of the outcrop, and the scale ruler is 20 cm. (A) Alternating layers of parallel-stratified, wave-worked sand and fine gravel, coarse gravelly debrisflow and debrisfall deposits, and units of intercalated mud, silt and very fine sand of tidal origin; note the ice-rafted dropstone (IRD) and the truncated overturned fold (arrow) attributed to slumping. (B) Backset of upslope-dipping tangential cross-strata above a concave-upward scour surface (arrow), representing an upper-slope chute filled with gravelly sand. (C) Parallel-stratified, wave-worked sand onlapping a slight erosional unconformity (arrow); the emplacement of large pebbles and cobbles is attributed to episodic debrisfall from a higher beach zone. (D) Successive packages of parallel-stratified, wave-worked sand and fine gravel with scattered spherical cobbles and an intervening debrisflow deposit, separated by truncation surfaces (arrows) attributed to storms; the varying inclination of strata reflects changes in their dip direction. Note the upslope imbrication of pebble blades in the lower two packages and the sand layers with ripple cross-lamination in the upper package. (E) Wave-worked, granule-rich coarse sand with gravel spheres and large blades, separated by a layer of medium to fine sand with wave-ripple cross-lamination; the fining- to coarsening-upward motif reflects changes in wave energy. (F) Debris-flow deposits composed of berm-derived gravel (medium to large discs and blades mixed with small spheres, blades and rods), separated by a slump deposit composed of alternating mud, silt and sand with seaweed patches (arrows). Note the sigmoidal, steepening- to flattening-upward fabric of dip-aligned clasts in the debrisflow beds. (G) Wave-worked, coarse to medium sand with flat-lying pebbles and cobbles (mainly discs and blades), overlain by a parallel-stratified fine sand with scattered granules that passes rapidly upwards into stratified, granule-rich very coarse sand with scattered pebbles, commonly imbricated in an upslope direction (arrow).

sediment was probably related mainly to the weak intrastratal horizons of seaweed material and/or mud, which tended to yield under the growing load and acted as a lubricating sole smear. This facies constitutes 17 vol.% of the fan-delta foreset unit in the proximal log 1 (Fig. 6) and 13 vol.% in the distal log 2 (Fig. 7).

The delta foreset architecture

The spatial distribution of facies in the fan-delta foreset succession indicates that the subaqueous slope of the prograding delta was increasingly wave worked with time and distance, evolving from massflow dominated and wave influenced into virtually wave dominated (Figs 6 and 7). The topset alluvium pinches out in the fan-delta middle reaches (Fig. 4, top), *c.* 920 m from the fan apex, and the subsequent seaward progradation of the delta foreset by *c.* 160 m was apparently caused by wave action combined with abundant sediment supply by longshore drift. A similar mode of foreset accretion, without fluvial supply, was described by Massari (1996). The change implies that the fluvial system either ceased to be active or became weak, incapable of wide sediment dispersal and possibly confined to the fan's northern flank.

No fossil fauna has been found in the poorly exposed proximal part of the fan-delta foreset unit, but the proximal/medial transition and medial to distal part contain shells of *Mytilus edulis*, a bivalve species known to have populated Svalbard coastal waters between 9·5 and 3·5 ka BP (Salvigsen *et al.*, 1992). Other fossils include *Balanus* sp. and the transported seaweeds. Silt and fine sand locally contain laminae of concentrated coal detritus, 0·5–2 mm in size, apparently derived from the coastal outcrop of the coal-bearing bedrock succession. The radiocarbon dates of 13 shell samples collected along the foreset outcrop section (Fig. 4) span a time interval from 6·2 ka to 4·9 ka BP (Table 1) and indicate that the mean progradation rate of the fan delta was high, but decreased markedly with distance: from 0·31 m $year^{-1}$ in the proximal/middle part to 0·13 m $year^{-1}$ in the wave-dominated distal part, and to 0·08 m $year^{-1}$ at the final stage (Fig. 10).

The foreset beds are dipping mainly at 25–33°, but the entire progradational succession abounds in internal unconformities (storm erosion surfaces) inclined at 10–30°, which are planar or gently curved, convex or concave upwards, and are either steeper or gentler than the underlying beds (Fig. 5A and B). The internal architecture of the wave-worked medial to distal foreset unit reflects the controlling role of wind and tides, the two independent causes of foreshore wave-energy fluctuations and swash stratification cyclicity (Allen, 1982, p. 468). The repetitive coarsening- and fining-upward bedsets (Fig. 9A), 12–27 cm thick, may reflect the gradual changes in wave energy related to neap–spring tidal cycle, combined with the more abrupt random changes resulting from variation in wind power and punctuated by storms. The bedsets consist of alternating sandy and gravelly layers (Fig. 9B), the former showing parallel stratification and shoreward cross-lamination, attributed to a preferential deposition by swash during tidal flood phases, and the latter showing shoreward-imbricated pebbles and attributed to preferential deposition by backwash during tidal ebb phases.

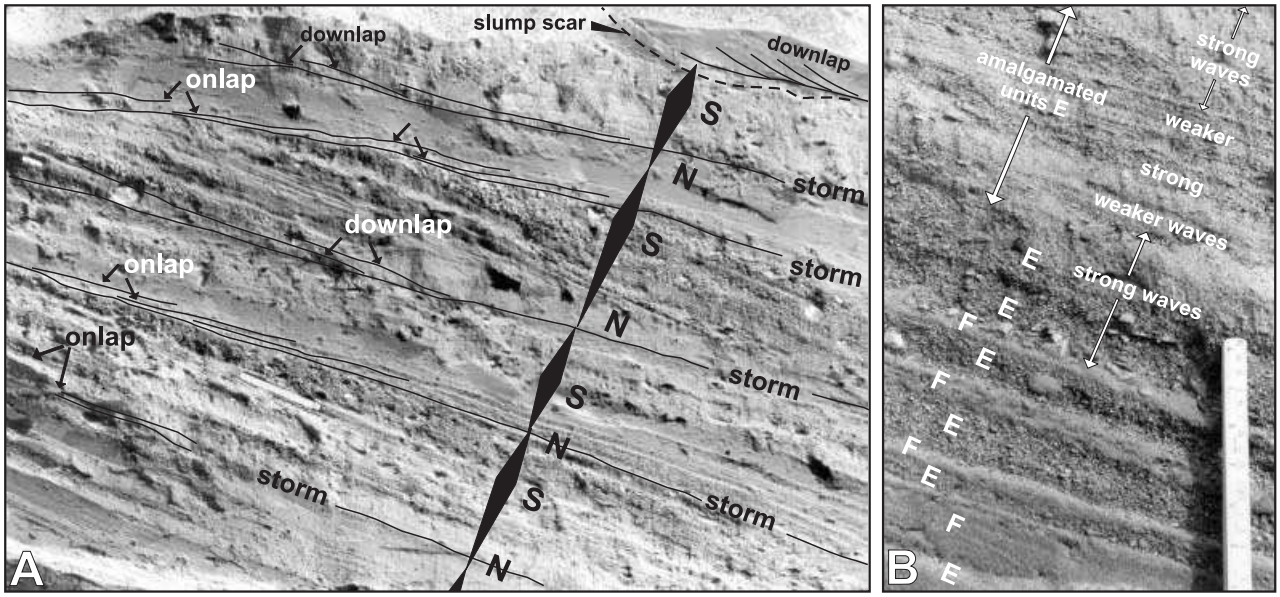

Fig. 9. Internal architecture of the fan-delta foreset unit (details from the distal part of the outcrop section in Fig. 4). (A) Textural and structural changes attributed to neap (*N*) and spring (*S*) tidal cycles punctuated by storm erosion; the coarsening- to fining-upward motif reflects gradual changes in wave impact, unrelated to storms, whereas the downlap or onlap of strata reflects the morphology of storm-formed surfaces, whether broadly cuspate or scoop-shaped. The ruler is 20 cm. (B) Detail of the coarsening-upward part of a *N*–*S* cyclothem, showing textural changes attributed to semi-diurnal flood (*F*) and ebb (*E*) cycles combined with wind-driven changes in wave energy; note that the coarser (spring-phase) part of the cyclothem, with shoreward-imbricated clasts, consists chiefly of the amalgamated backwash deposits of ebb-time waves, modulated by changes in wind power. The ruler portion is 15 cm.

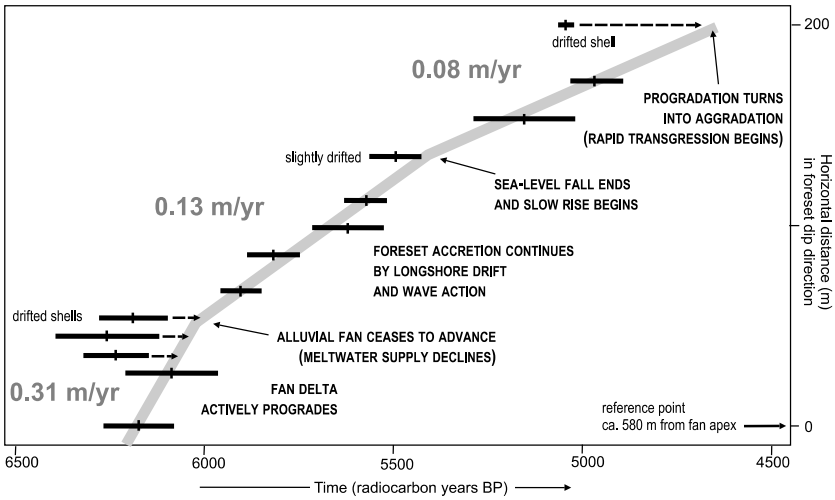

Fig. 10. An interpreted plot of the radiocarbon dates vs. the true, dip-parallel horizontal distance of delta foreset advance (data in Table 1), serving as an estimation of the changing rate of fan-delta progradation. The progradation involved an abundant supply of sediment by longshore drift, hence the 'too old' dates of some of the shells (redeposited).

The coarse, spring-tide part of a cyclothem (Fig. 9B, top) consists of amalgamated backwash (ebb-phase) deposits, varying texturally due to irregular fluctuations in wind power, with few swash layers preserved. The repetitive occurrence of isolated muddy units, interspersed with fine-grained tidal ebb deposits (Figs 6 and 7), is interpreted to be the record of the winter shoreline conditions in an ice-covered, wave-free fjord.

On a longer time scale, this composite record of different controlling factors has been heavily distorted by the 'random noise' introduced by storm erosion, slumping and massflow events, particularly common in the proximal to medial part of the fan-delta foreset unit. The foreset truncation surfaces (Fig. 5A and B), representing storm events, are overlain conformably (Fig. 8D), downlapped or onlapped (Figs 8C and 9A) by the

wave-worked sediment deposited during the post-storm recovery of the fan-delta face. These diverse stratal patterns of slope reactivation reflect the local gradient and morphology of the storm-formed surface, whether planar, broadly cuspate or scoop shaped (Caldwell & Williams, 1985; Massari & Parea, 1988; Sherman *et al.*, 1993; Bluck, 1999). Planar and moderately inclined surfaces tend to aggrade by vertical accretion (stratal toplap), beach cusps prograde by seaward accretion (downlap), whereas the scoop-shaped intercusp embayments are backfilled by aggradation (onlap).

The fan-delta foreset succession also abounds in isolated trough-shaped scours, 30–70 cm deep, trending downslope and shallowing out in both downslope and upslope directions. These are commonly filled with a backset unit of upslope-dipping tangential cross-strata of pebbly coarse sand and/or fine pebble gravel (Figs 5A and 8B). These features are thought to be short chutes, or plunging furrows, scoured by storm-generated rip currents and often filled by the current subject to a hydraulic jump (Nemec, 1990; Massari, 1996; Nemec *et al.*, 1999; Lønne *et al.*, 2001). Although a reflective shoreline normally lacks such jets of seaward-returning water, they can be generated briefly by storms when the coastal setup renders the shoreline dissipative (Gruszczyński *et al.*, 1993). Other isolated backsets, composed of granule-rich pebbly sand and overlying apparently non-erosional surfaces, are probably swash bars accreted to the delta face during its post-storm recovery in high wave-energy conditions (Hobday & Banks, 1971; Fitzgerald *et al.*, 1984; Massari & Parea, 1988; Briseid, 1994).

A conspicuous feature of the fan-delta foreset unit is the lack of recognizable mouth-bar wedges, which are commonly preserved in both glacial and non-glacial Gilbert-type deltas in lower latitude coastal settings (Postma & Cruickshank, 1988; Colella & Prior, 1990; Nemec *et al.*, 1999). Their lack in the present case reflects a marked disequilibrium between the strong and longer lasting wave action and the ephemeral, moderate to low stream discharges.

Fig. 11. Fan delta-front beach facies. (A) Beach-ridge gravel overlying and interfingering with the delta foreset deposits in a proximal outcrop of the fan delta; note the local abundance of stream-derived submature gravel in the beach unit; the ruler is 20 cm. (B) Beach-ridge succession in a medial part of the fan delta, comprising an accretionary gravel berm (*b*) with large oblate clasts arrested at the toe and with pebble sheets spread as selection pavements over a sandy beachface (*a*); fine gravel wedge (*c*) accreted in the shadow of an erosional berm as a seaward-protruding cusp armoured with large discs/blades; a washover wedge of pebbly sand (*d*); and coarse gravel (*e*) accreted during a high-tide reactivation of the earlier landward berm. The direction of delta-front progradation is obliquely to the right, at *c.* 60° out of the outcrop, and this local succession is probably a result of storm activity over two neap–spring tidal cycles (cf. Bluck, 1999, Fig. 9); the lens cap is 5 cm. (C) Beach-ridge gravel in a distal part of the fan delta, showing distinct size and shape sorting: (*a*) beachface sand with pebbly selection pavements, including large spheres; (*b*) coarse pebble gravel dominated by discs/blades, filled with sand, granules and small pebble spheres and containing isolated oblate cobbles; (*c*) sand-rich, fine pebble gravel dominated by spheres and rods; (*d*) sand-filled, coarse pebble gravel dominated by discs/blades, with subordinate spheres; (*e*) granule gravel with scattered spherical pebbles; (*f*) sand-filled, fine pebble gravel dominated by spheres and rods, with scattered large pebble discs/blades; (*g*) sand-filled, coarse pebble gravel dominated by spheres and rods, with scattered cobble discs/blades. The direction of delta-front progradation is towards the viewer; the pen is 14 cm. (D) Cross-stratified backshore runnel sand intercalated with storm washover gravel and overlain by alluvium; the direction of delta-front progradation is obliquely to the right, at *c.* 45° out of the outcrop, whereas the direction of sand transport is perpendicular, at *c.* 40° into the outcrop; the ruler is 20 cm. (E and F) Isolated wedge-shaped clusters of steeply inclined discs/blades within the berm framework of disorderly or gently inclined clasts. (G) Sand-dominated beachface facies overlain by beach-ridge gravel in a distal part of the fan delta, showing a storm truncation surface (*a*); deformed low-tide (*b*) and high-tide beach cusp (*c*); washover sand (*d*) behind a neap-phase berm; accretionary spring-phase berm (*e*); and a sand-rich gravel shadow (*f*) of spring-phase erosional berm. The direction of delta progradation is obliquely to the right, at *c.* 30° out of the outcrop; the steep, bulldozed clast fabric (arrows) is attributed to deformation by sea ice pushed against the beach.

Delta-front beach facies

The foreset beds of the fan delta pass updip into, and interfinger with, a subhorizontal gravel unit (Fig. 11A) that commonly exceeds 1 m in thickness and is clearly an integral part of the prograding delta front (Figs 4 and 5A and B). These gravelly deposits virtually replace the foreset facies near the distal end of the fan delta (Fig. 5C), but are lacking in its proximal part, where they were either not deposited or, more likely, eroded by the fluvial distributary system. The unit consists of clast-supported, pebble and cobble gravel, mainly subrounded to rounded, filled with a mixture of sand, granules and small pebbles, generally better rounded, but much poorer sorted. Stratification is poor,

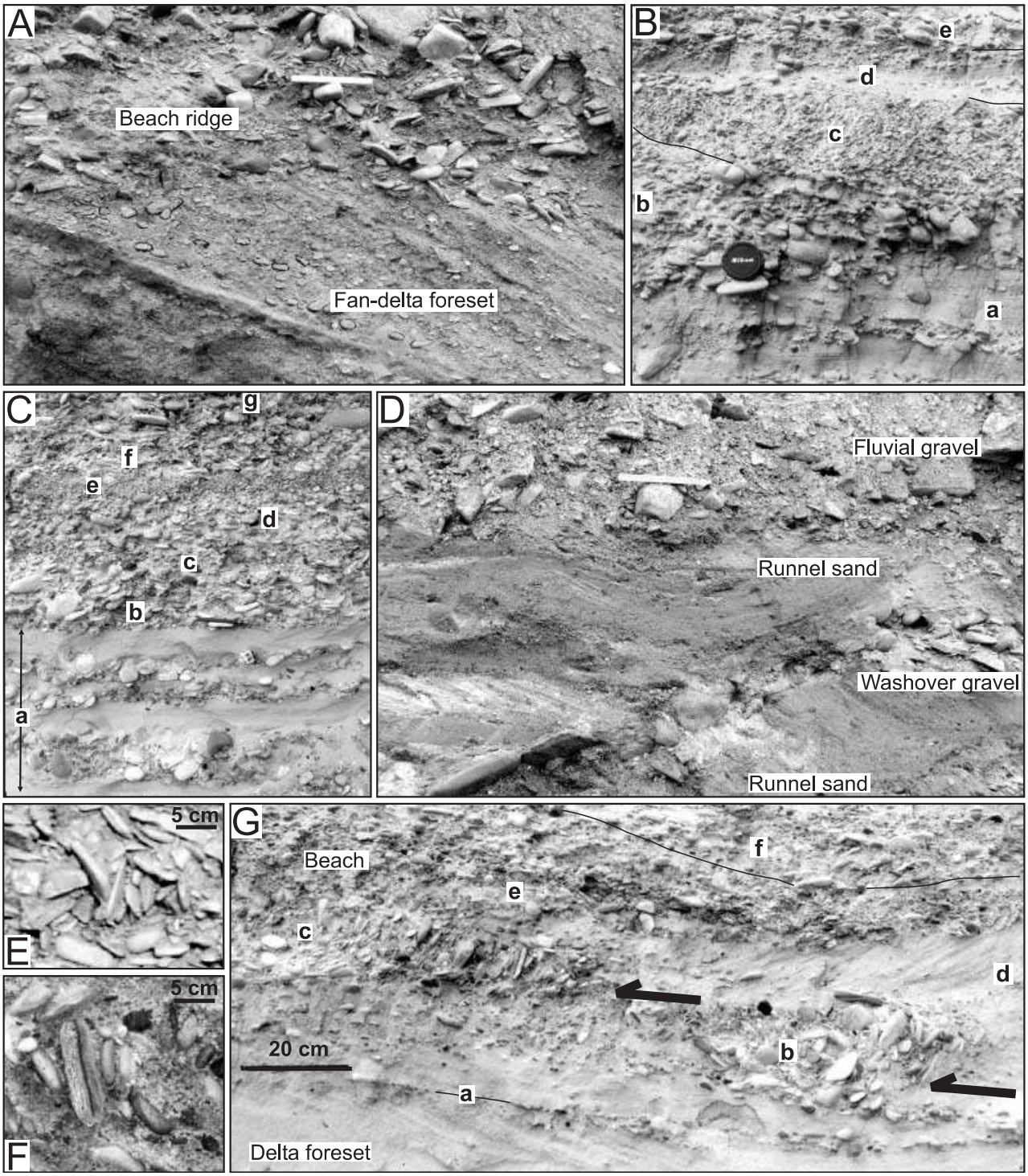

but the gravel shows thick subhorizontal layering with common evidence of size and shape sorting (Fig. 11B and C), as is characteristic of beach deposits (Bluck, 1999). Some interlayers consist of granule gravel. In the proximal part of the outcrop section, the gravel unit locally contains lenses of granule-rich, cross-stratified sand with shore-parallel transport directions (Fig. 11D). Large clasts in the upper part of the gravel unit are mainly subhorizontal and crudely aligned with the delta-front strike, but are commonly normal to the strike and dipping either seawards or landwards in the lower part. The framework of chaotic or gently inclined clasts contains isolated, wedge-shaped clusters of nearly vertical, small cobble discs and blades (Fig. 11E and F). The basal part of

the gravel unit locally shows short deformation zones, where clasts have been steepened, piled landwards into subvertical positions by a tangential force (Fig. 11G).

This gravelly facies shows typical features of beach deposits (Massari & Parea, 1988; Williams & Caldwell, 1988; Postma & Nemec, 1990; Bluck, 1999) and indicates that the fan-delta advance was accompanied by the formation and concurrent seaward migration of a delta-front beach ridge, or accretionary berm complex. The berm was apparently deposited by storm breakers, controlled by tides (cf. Fig. 11B), and formed an extensive, regressive beach platform. The lenses of cross-stratified sand are backshore runnel deposits, only locally preserved. The wedge-shaped clusters of steep, edgewise clasts (Fig. 11E) were probably formed by lodgement under the impact of storm waves, possibly combined with a tidal current (Sepkoski, 1982; Whisonant, 1987). When loose clasts slide along the substrate, some of them may rotate and be pinned in a near-vertical position by interacting with others and, as these edgewise clasts increase the substrate roughness, other pivoting clasts tend to be wedged steeply between them (Mount & Kidder, 1993). Clusters wedged in sandy gravel (Fig. 11F) may have formed by the breakdown of an imbricate fabric caused by 'sand flooding' and loss of substrate permeability (Bluck, 1999). The local occurrence of landward-bulldozed gravel (Fig. 11G) is attributed to a contemporaneous deformation by slabs of coastal ice pushed onto the beach at high tide. The preservation potential of such a deformed fabric on a wave-dominated beach is low, hence these features are rare. The scarcity of landward-inclined washover strata (Figs 4 and 5B) is consistent with the regressive nature of the beach platform. The delta foreset near the distal end of the outcrop section (Fig. 4, bottom right) apparently ceased to advance around 4·7 ka BP (Fig. 10), turning into an aggradational gravelly beach (Fig. 5C) that recorded the onset of a rapid marine transgression.

Alluvial topset facies

The fan-delta topset unit (Figs 4, top, and 5A) is up to 4 m thick, has an uneven, erosional base and consists mainly of cobble to boulder gravel. Its upper surface is even more irregular, incised by isolated younger fluvial channels and covered erosionally by marine deposits in the pinchout zone of the topset unit (Fig. 4). Palaeochannels are poorly recognizable, multilateral and amalgamated, mainly 5–10 m wide and 0·8–1·2 m deep (Fig. 4, top). The channel-fill gravel commonly shows a crude upward fining (Fig. 6, right) or consists of multiple units, 20–40 cm thick, each weakly coarsening upwards. The coarse gravel has a clast-supported framework filled with pebbles and sand, but is poorly sorted and subangular to subrounded. Clast fabric varies on a local scale: large discs and blades are mainly subhorizontal, whereas the medium and small clasts are more randomly oriented, often subvertical, entrapped between the large ones and locally imbricated in an upfan direction. A longitudinal outcrop section (southern escarpment of sector 2, Fig. 3A) shows a crude alignment of coarse tabular clasts along subhorizontal or gently inclined surfaces, indicating a combination of vertical and downstream accretion. High-angle cross-stratification is generally lacking. The transverse and oblique sections of palaeochannels (Figs 4, top, and 5A) show multiple scours and subhorizontal to inclined gravel layers, indicating aggradation combined with unilateral or bilateral accretion.

The amalgamated palaeochannels filled with coarse gravel, including boulders up to 160 cm in size, indicate shallow, but powerful, laterally shifting braided streams. The fining-upward channel-fill motif probably reflects aggradation and decreasing channel capacity. The crude stratification and coarsening-upward motif suggest gravel accumulation in the form of expanding, low-relief longitudinal bars and bank-attached side bars (Boothroyd & Ashley, 1975; Church & Jones, 1982; Nemec & Postma, 1993). The poorly organized fabric reflects the poor sorting of the gravel and a high stream-floor roughness. The clasts were probably sliding individually in short jerky motions, rather than rolling in groups and adjusting to one another, and hence were prone to pivoting and random interstitial lodgement. Local lenses of unsorted gravel, 20–70 cm thick, with a steep clast fabric similar to that shown by modern debrisflow deposits (fan sector 2), are thought to be erosional relics of debrisflow mounds emplaced in the stream channels (Fig. 6, top right). The evidence as a whole indicates that the deposition of the fan-delta topset alluvium involved processes and bedforms resembling those observed in the active modern part of the fan (sector 2), discussed in a subsequent section.

Transgressive spit facies

This gravel unit, around 1 m in thickness, overlies the delta-front beach platform and distalmost

topset alluvium (Figs 4 and 5), at least in the exposed eastern half of the fan delta. The unit consists of a single foreset of tangential to sigmoidal cross-strata (Figs 5 and 12) inclined at an angle of up to 40° northwards, in an upfan direction. The uneven base of this foreset unit rises in the same direction, clearly onlapping the fan-delta plain (Fig. 4), and varies between erosional and depositional (Fig. 12). The cross-strata are defined by an alternation of fine and coarse pebble gravel, the former rich in large platy pebbles and the latter including platy and oblate cobbles (Fig. 12). Cobble blades and discs are commonly imbricated relative to the cross-strata, inclined in an updip direction, apparently due to sliding on the foreset slipface. The gravel framework is clast supported and filled with sand. Large pebbles and cobbles are mainly subrounded and disc or blade shaped, whereas the fine gravel is rounded and abounds in spheres, although shows little shape sorting. No fossil fauna has been found in this unit, but the textural maturity of the gravel and the landward inclination of cross-strata indicate accretion by marine processes.

The textural characteristics indicate wave-worked gravel of beach provenance, and the landward dip of the cross-strata and rising base imply a marine transgression. This gravelly unit is thought to represent an advancing spit formed by storm washover processes (Kraft *et al.*, 1978; Nicholls & Webber, 1987; Carter *et al.*, 1990; Hiroki & Masuda, 2000), somewhat similar to the spit forming at the present-day shoreline (see later discussion and corresponding Fig. 15A and B). The spit climbed onto the drowning fan-delta plain over a horizontal distance of at least 195 m in the cross-strata dip direction and reached an altitude of *c.* 6 m (Fig. 4). The advancing spit buried the associated backshore zone, the latter varying between erosional (runnel) and non-erosional, which explains the uneven base of the gravel unit. Sporadic mud lenses embedded in the gravel unit represent minor, short-lived lagoons. The transgressive spit platform has an uneven upper surface with strike-parallel swales and shallow troughs, probably some incipient berms and relic runnels formed during regression, and is erosionally overlain by younger alluvium (isolated palaeochannels). Some of the surficial depressions are filled with non-fossiliferous, gravel-bearing muddy sand, attributed to subaerial sheetwash.

Surficial post-spit alluvium

The inactive surface of sector 1 (Fig. 3A) shows a radial pattern of palaeochannels and ridges of relic debrisflow deposits, obliterated by sheetwash and thinly covered with soil and vegetation. Some palaeochannels are visibly fresher than others. A wide and relatively fresh axial palaeochannel, with margins slightly obliterated by sheetwash and oblique runoff, extends from the fan apex to the edge of the modern shoreline escarpment (Figs 1B and 3A), where it is less than 0·7 m deep, hanging at the top of the outcrop section (Fig. 4, top left). In the eastern half of the fan delta, the radial linear features are increasingly diffuse below an altitude of 20 m (Fig. 3A), where recognizable palaeochannels are fewer and

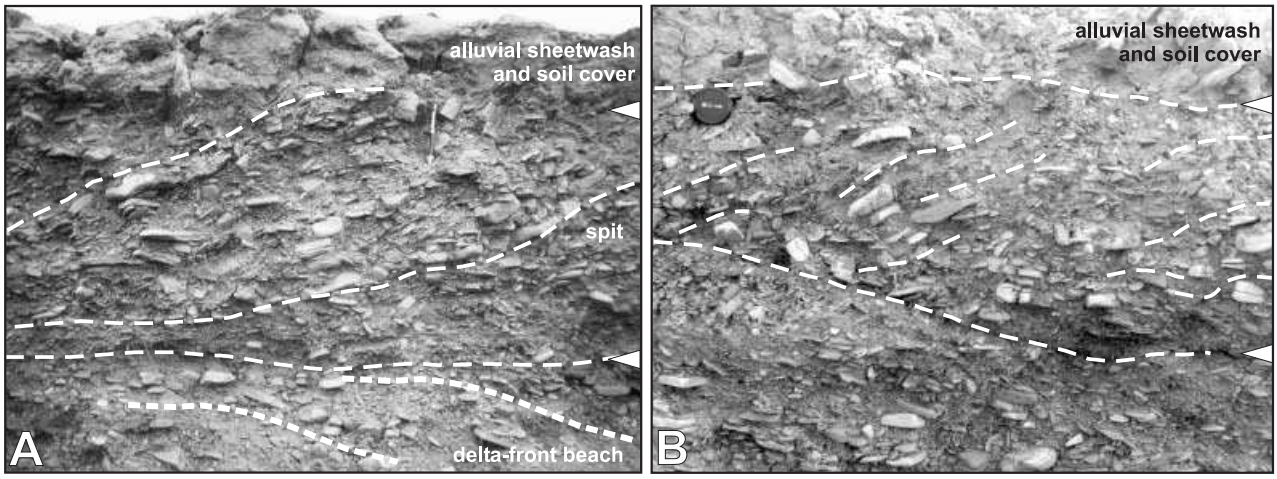

Fig. 12. Transgressive spit gravel overlying the regressive delta-front beach deposits; the lower boundary of the spit platform unit indicates a variable, non-erosional (A) to erosional onlap (B) onto the fan-delta plain. The pen is 15 cm and the lens cap is 5 cm; seaward direction is obliquely to the right, at *c.* 30° out of the outcrop.

a sheetwash layer of gravel-bearing muddy sand (Fig. 7, log top) has smoothed out the surface, also partly covering the raised beach at the northern rim of Moskuslaguna (Fig. 3A, dotted zone). The abandoned fan surface has clearly been modified. For example, the 1936 aerial photograph (Fig. 1B) shows a south-trending palaeochannel, *c.* 20 m wide and more than 1 m deep near the apex, which has been obliterated by 1990 (Figs 3A and 13A).

The surficial palaeochannels are relatively wide and shallow (Fig. 4), filled with a poorly sorted, subangular to subrounded pebble and cobble gravel, locally underlain by a bouldery lag. The crude coarsening-upward gravel units, 0·2–0·5 m thick (Fig. 7, near log top), with weak stratification marked by subhorizontal layering of clasts, suggest longitudinal bars, similar to those observed in the active sector 2 (described in next section). High-angle cross-stratification is absent. In the upper to middle fan reaches, many of these gravel-filled, ribbon-like palaeochannels have a positive surficial relief, which implies their partial exhumation by subsequent water runoff and sheetwash erosion.

The surficial post-spit alluvium indicates that the fluvial distributary system operated mainly as a solitary channel, shifting widely and occasionally extending to the lower fan reaches, thereby crossing the emerged platform of transgressive spit deposits. This evidence supports the notion of reduced fluvial activity and indicates a rapid fall in relative sea level. The regressive shoreline shift clearly outpaced fluvial sediment dispersal, and the wandering stream was eventually entrapped by incision on the fan northern flank (Fig. 3A), while the abandoned fan surface continued to be modified by episodic sheetwash processes.

Post-spit regressive beach facies

These fossiliferous gravelly deposits at the distal end of the fan-delta section (Figs 3B and 4, bottom right) erosionally overlie the transgressive spit platform, although they are rather poorly exposed in this low, outermost part of the shoreline escarpment (Fig. 1B). The deposits form a foreset of convex-upward, gently seaward-inclined (< 20°) strata of alternating pebble and granule gravel with common intercalations of coarse to very coarse sand that is mainly granule rich and parallel stratified. Cobble discs and blades abound at the top of the foreset, whereas large spheres are scattered along the inclined accretionary strata. The gravel consists of mainly subrounded and rounded clasts, shows evidence of shape sorting and generally resembles the delta-front beach facies described earlier in the text. A radiocarbon date from the earliest, landward part of these deposits (sample T-13358 in Table 1) indicates that they are considerably younger than the original distalmost deposits of the fan delta. Only the upper part of this young foreset unit is exposed (Fig. 3B). It passes distally, seawards, into the modern beach deposits of similar grain-size range and, laterally, into a raised strandplain at the northern rim of Moskuslaguna (Fig. 3A).

The gravel texture and stratification pattern indicate a raised accretionary beach formed during a relative sea-level fall. The radiocarbon date indicates that the falling sea level reached an altitude of *c.* 1·7 m around 4·3 ka BP (Fig. 4, bottom right). Except for this distalmost part of the outcrop section, the regressive shoreline shift deposited little or no sediment over the pre-existing, transgressive spit platform, which suggests a rapid regression that was initially non-depositional. The re-emerging fan delta was probably swept by longshore currents, although the lack of regressive marine deposits may also be attributed partly to subsequent subaerial erosion. The accretionary beach passes seawards into the modern strandplain at the outer fringe of the fan delta, which indicates that the rate of the forced regression declined after the relative sea level had fallen by more than 4 m and slowly began to approach its present-day position.

Sedimentation in sector 2

The narrow, active sector 2 of the fan delta (Fig. 1B) has an angular width of 25° and is up to 240 m wide in its lowest segment. It extends seawards as a depositional protrusion, *c.* 160 m in length and 345 m wide, over a strandplain accreted from the north-west to the delta front (Fig. 3A). This sector is incised, bounded by a bedrock escarpment on the northern side and an erosional terrace of the former alluvium of sector 1, up to 4 m high, on the south-eastern side (Fig. 3A). The island-like relics of this former alluvium in sector 2 (Fig. 13A) are isolated, vegetated terraces, mainly no higher than 2 m. The incision extends up to the fan apex, where the active sector is narrow and passes into a channel draining the slope catchment (Figs 1B and 3A). For the purpose of the ensuing description, the active sector has been divided into three subsectors (labelled 2a–c in Figs 3A and 13A) on the basis of its morphology and inferred chronology of main fluvial activity.

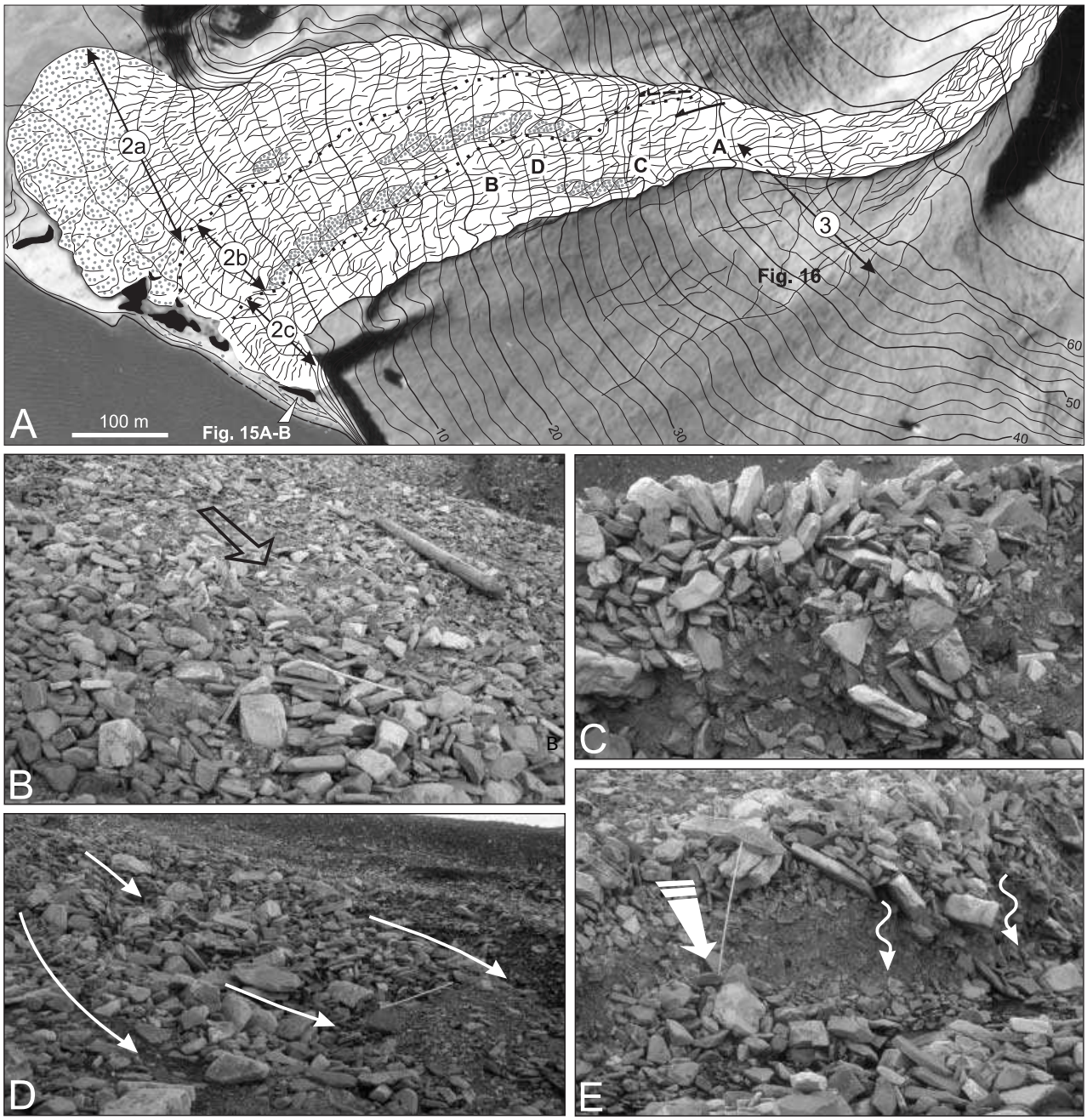

Fig. 13. (A) Overlay drawing on a portion of aerial infrared photograph (top), showing the active sector 2 of the fan delta in 1990 (Norwegian Polar Institute, S90-5402). The densely dotted 'islands' are relic terraces of the former alluvium of sector 1 (cf. Fig. 3A), whereas the dotted distal lobes are terminal splays of water-laid pebbly sand. Letters B–E indicate the approximate location of the close-up details shown by the photographs below. (B) Frontal part of tongue-shaped debrisflow deposit emplaced in stream channel and winnowed by surficial water flow; note the steep, flow-transverse fabric of tightly packed platy clasts; the white ruler is 1 m. (C) Stream-undercut flank of a debrisflow deposit, 1·35 m thick; note the steep fabric of platy clasts and the water-winnowed upper part of the matrix-bearing gravel; downstream direction to the left. (D) A lee wedge of gravelly sand formed by the winnowing of matrix and gravel clasts from a debrisflow deposit; the ruler is 1 m. (E) Stream-undercut flank of a debrisflow deposit, the matrix of which has been increasingly winnowed by percolating water (thin arrows), and the framework gravel collapses on the stream floor (thick arrow); downstream direction is to the left and the ruler is 1 m.

Alluvial fan incision reflects a state of erosional degradation, whereby a stream channel cuts down into the fan and debouches beyond the fan margin, thus terminating the dispersal of sediment over the fan surface (Wasson, 1977). The stream channel in the present case was

apparently wandering across the fan surface during the latest regression (see the post-spit alluvium in Fig. 4) and eventually shifted to the low-lying northern flank of the fan, where it was entrapped by incision instigated by erosional shoreline retreat (i.e. its recession from the maximum seaward extent to present-day position, Fig. 3A). The supply of sediment from the catchment continued, including incursions of debrisflows and debris-bearing sporadic snow avalanches, and the ephemeral stream has been struggling between the necessity to distribute the sediment and the need to adjust its own profile to the receding shoreline. The modern stream has had a limited capacity to cope with the coarse sediment, supplied episodically in large portions, whereby net aggradation often prevailed in the short term, causing the stream to shift laterally and widen the active sector.

The sector's low-lying surface accumulates snowdrift, particularly in the wind shadow of the southern escarpment. As the runoff begins in early summer, this thick local snowpack causes the meltwater flow to concentrate in subsector 2a (Fig. 13A). The stream here is unable to reach the shoreline, migrates laterally and transfers sediment to the lower reaches, which mainly causes aggradation. The flow then shifts gradually to subsector 2c later in the summer, when the local snowpack vanishes. The stream in this zone reaches the shoreline, which favours incision, although net aggradation often prevails on a seasonal basis. Subsector 2b is a transit zone for the stream migration, as competing erosion and deposition repeatedly cause the stream to cross this area. The meltwater forms a shallow, poorly defined, unstable channel with a braided thalweg and primitive longitudinal bars. The uneven and rapidly changing morphology of sector 2, particularly in its proximal part, reflects a strong disequilibrium between the stream's limited hydraulic power and a morphodynamic requirement to degrade its profile. The stream has been forced gradually to erode its own deposits, the original fan-delta alluvium and the channel-plugging mounds of contemporaneous debrisflow deposits, all of which are composed of coarse gravel.

The debrisflows descend from the catchment slopes through the fan-head channel. They consist of cobble and boulder gravel, angular and mainly platy in shape, supported by moderate amounts (15–30 vol.%) of muddy sand matrix, generally rich in pebbles and possibly containing slush. It is the fine-grained watery matrix that lubricates the mass of low-mobility debris. The debrisflows form tongue-shaped mounds, typically 4–8 m wide and 0·5–1·5 m thick, with a steep clast fabric forming a horseshoe pattern and a tail of levee ridges (Fig. 14A, 1). The clasts tend to be piled steeply (Fig. 13C and E), assuming a transverse orientation within the debrisflow front and body and a flow-parallel attitude along the flanks and levees (Fig. 13B). The stream then gradually dismantles the gravel mound over successive summer seasons.

As the debrisflow mound plugs the stream channel, the flow of water is focused in the interlevee trough and along the mound flanks and upper surface (Fig. 14A, 1). The water washes out the matrix (Fig. 13B and C) and undercuts the flanks, which then keep losing matrix and collapse (Fig. 13E). The removed sand and gravel form a lee wedge (Figs 13D and 14A, 2), while the winnowing increases the mound surface roughness and intensifies flow turbulence. Increasingly more gravel is swept onto the lee wedge, including clasts that collapse from the eroded flanks and are carried downstream, which causes the wedge to grow and evolve into a primitive longitudinal bar (Fig. 14A, 3, and B). The bar may develop a crude coarsening-upward trend (Fig. 14C), indicating progradation (Nemec & Postma, 1993), although the bar head is an immobile relic of the parental debrisflow deposit. The bar broadens, becomes increasingly armoured with large clasts and reaches maturity,

Fig. 14. (A) Schematic plan-view cartoon (diagrams 1–4) showing how a debrisflow gravel mound (DF), emplaced in a stream channel (S) and tailed with levees (L), affects the stream flow and is gradually dismantled by the latter. A thin lee wedge (LW) of stream-winnowed sand and gravel is formed and evolves into a head-pinned longitudinal bar (LB), while the mound flanks are undercut; the bar becomes armoured with large clasts, stabilizes, and crude transverse ribs (TR) may form on its surface, while the gravel swept along one or both of the flanks forms another longitudinal bar; relic levees often survive as longitudinal ridges (R). The photographs show details from fan sector 2. (B) Lobate longitudinal bar on the lee side of a stream-eroded debrisflow deposit. (C) Vertical outcrop of a longitudinal bar dissected by a stream, showing tractional fabric and crude upward coarsening; downstream direction is to the left. (D) A secondary longitudinal bar formed on the stream-eroded flank of an immobile primary bar; note the lobate bar shape and downstream fining. (E) Relic debrisflow levee, composed of steeply flow-aligned coarse gravel, preserved as a longitudinal ridge in a stream channel; downstream direction is away from the viewer.

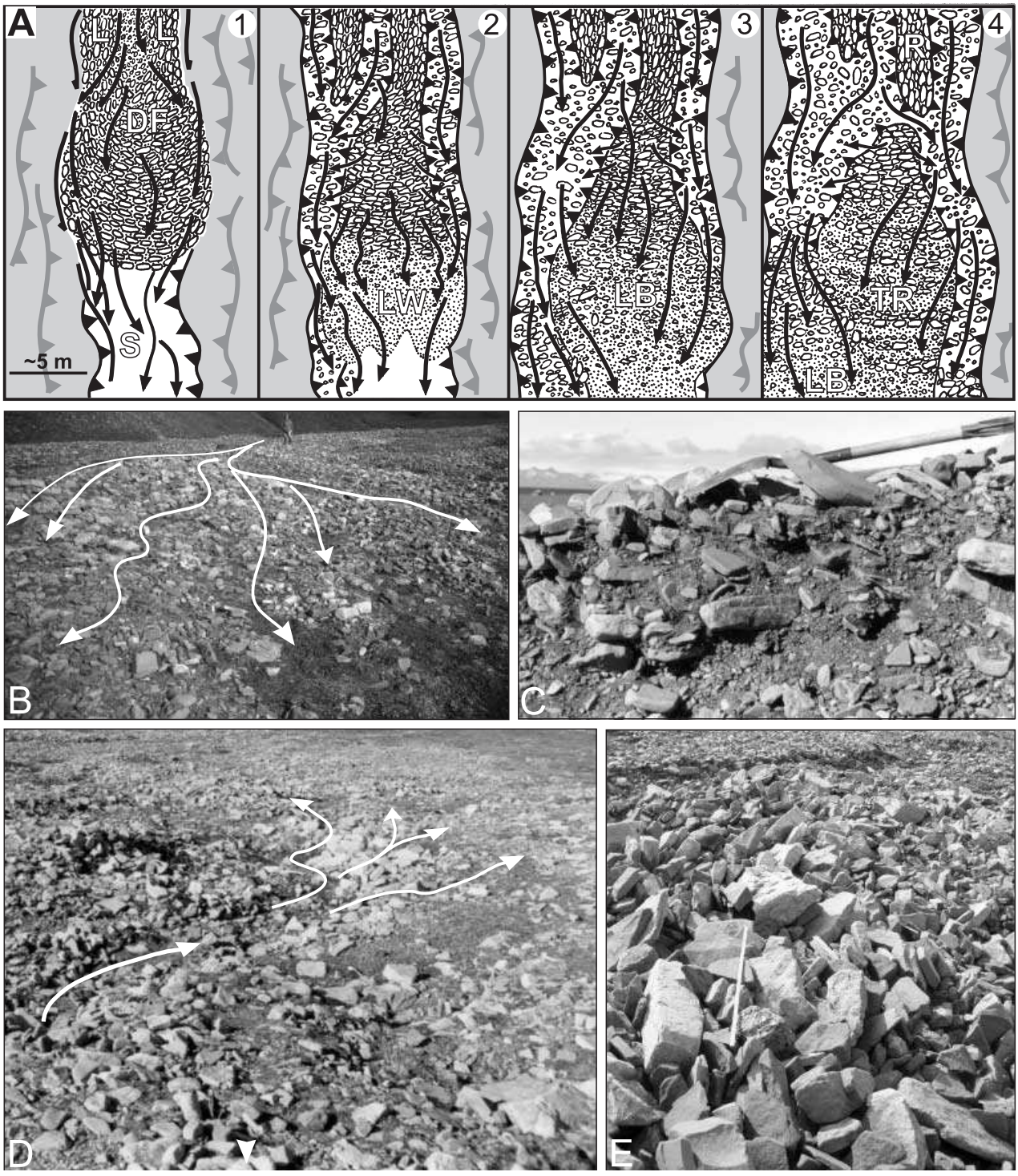

when crude transverse ribs (Koster, 1978) may appear on its surface (Fig. 14A, 4). Meanwhile, the gravel swept along the bar's eroded flank accumulates at a downstream site of flow expansion, forming another longitudinal bar (Fig. 14A, 4, and D), composed solely of water-laid gravel and potentially more mobile. The original debrisflow deposit thus gradually vanishes, although one or both of its levees often survive as relic longitudinal ridges (Fig. 14E), owing to the gravel coarseness and flow-parallel steep fabric; the ridge is subsequently refilled with sand and fine gravel and becomes temporarily buried when the formation of bars instigates upstream aggradation.

Subsector 2a terminates in a broad accumulation of shingled, water-laid sandy splays (Fig. 13A), extending over the strandplain and onlapping laterally the alluvium of subsector 2b. The younger splays have been deposited in a back-stepping manner over the earlier ones, presently vegetated in their distal part, which indicates seaward expansion, aggradation and gradual abandonment of this terminal zone. The gravelly sand is visibly fresh, little coated by lichen and is thought to have been washed out during the Little Ice Age maximum. The accumulation of snow increased at this time, and the southern half of sector 2 – most prone to snow-drift accumulation – was probably perennially occupied by a thick snowpack. The runoff would then be lower and limited to subsector 2a. Subsector 2c, the freshest and more incised, was probably established after this climatic episode, when the snow cover begin to vanish during the summer, the net water yield increased and the stream shifted away from the aggraded zone. The stream presently reaches the shoreline along the southern margin of subsector 2c. The stream-supplied sediment here is heavily reworked by waves, mixed with sediment derived by longshore drift and is persistently remoulded by storms into a spit ridge that blocks the stream outlet (Figs 13A and 15A and B).

It should be emphasized that the catchment's present-day meltwater yield is low and the stream discharges are very limited, but the frozen substrate and high bed roughness maximize the hydraulic effect. On an alluvial fan in a mid-latitude semi-arid region, a water flow of this magnitude would percolate into the coarse substrate and have little effect on sedimentation.

Modern shoreline sedimentation

The decline in sediment supply allowed the action of sea waves and longshore currents to prevail, with a major impact on the abandoned fan delta (Fig. 1B). The shoreline along three-

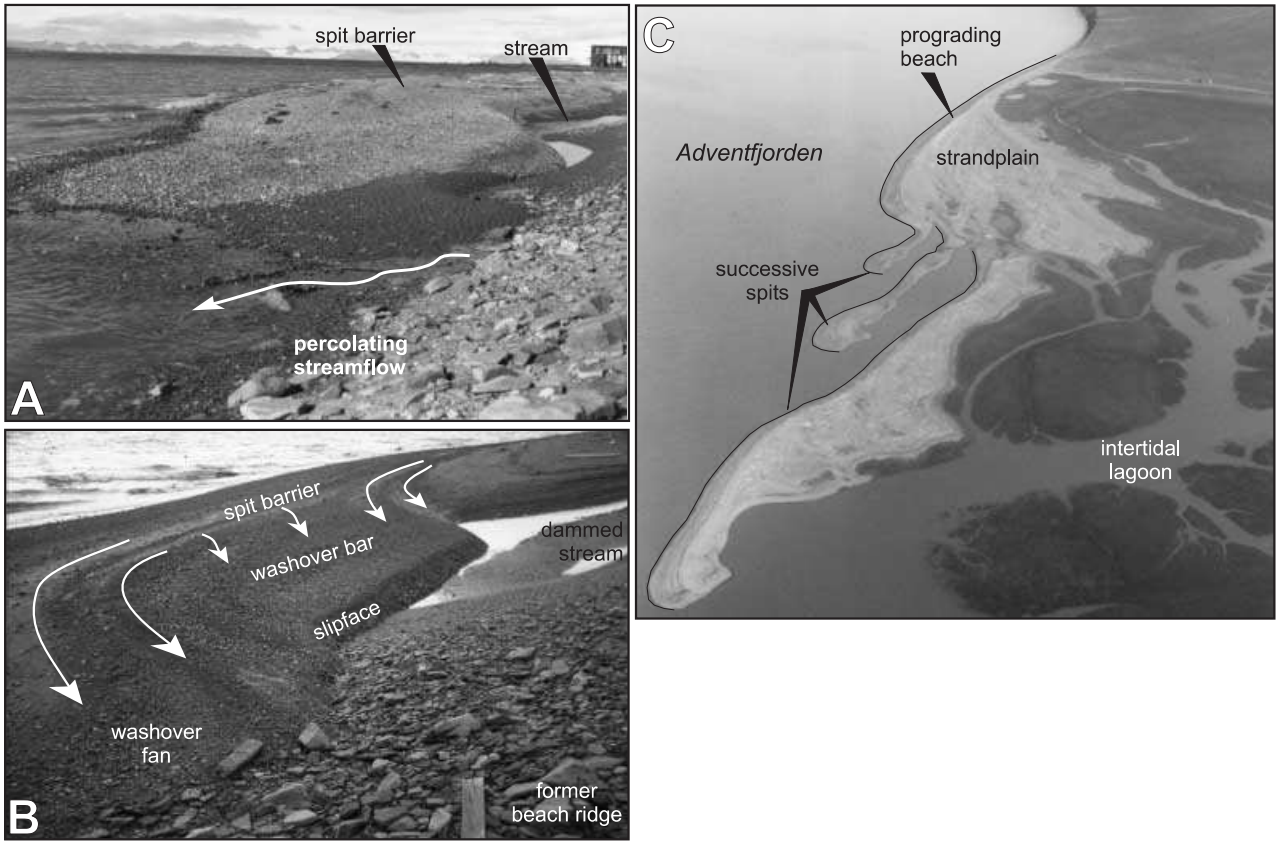

Fig. 15. (A) Modern spit ridge accreted to the north-western side of Hiorthfjellet fan delta and diverting the active stream in a shore-parallel direction (shoreline in sector 2c, Fig. 3A). (B) The same spit remoulded by a modest storm, with the washover deposits damming the stream outlet. (C) Modern spit complex accreted to the south-eastern side of the fan delta, sheltering the intertidal Moskuslaguna (cf. Fig. 1); note the welding of successive spits into a regressive, progradational strandplain. Photographs taken in July 1999.

quarters of the fan-delta perimeter has dramatically retreated as a result of wave erosion, evolving into a broad marine shoal rimmed with a seaward-concave escarpment (Fig. 3A). The sediment removed by the erosion has been drifted to the south-east by longshore currents, forming an accretionary spit complex that presently shelters the intertidal Moskuslaguna (Fig. 1). The successive spit ridges accreted to the margin of the eroded fan delta have merged into a prograding strandplain (Fig. 15C). The modern stream discharges are insufficient to compete with the marine processes, and the active sector 2 of the fan delta shows little evidence of recent progradation. The protrusion of outwash splays here occurred over a strandplain accreted laterally, from the north-west, to the wave-trimmed margin of the fan delta (Fig. 3A).

The recent erosional transgression of the fan-delta has thus been coeval with a normal, progradational regression along the coast lateral to the fan delta, on both its sides. This differential behaviour of the fjord shoreline reflects a strong morphodynamic disequilibrium resulting from the abandonment of the protruding fan delta by its declining fluvial system, which has led to a vigorous lateral transfer of sediment by the shoreline-smoothing action of marine processes.

Sedimentation in sector 3

The fan-head area defined as sector 3 (Figs 1B and 3A), *c.* 400 m in length and up to 210 m wide, shows clear evidence of a recent accumulation of fresh debris on the abandoned fan surface (Figs 13A and 16A). This modern active sector is an area of deposition, lacks incision and has an indistinct outer boundary. The deposits are patchy lobes of coarse angular gravel underlain and surrounded by a relatively thin layer of gravel-bearing muddy sand that is sparsely vegetated (Fig. 16B). The fan surface here is perched 1–3 m above the incised active sector 2 (Fig. 16A), and it is unlikely that this terrace area was ever flooded in recent times, especially by a water flow carrying cobbles and boulders. The area is also far beyond the reach of any possible rockfalls.

The characteristics of the deposits include: an uneven, patchy surficial distribution of coarse debris, with abundant large cobbles and boulders (Fig. 16B); a disorderly mixture of flat-lying and subvertical or imbricated boulders standing above ground level, many in metastable positions (Fig. 16C and G); and common pockets of fine gravel perched precariously atop the large boulders (Fig. 16D–G) or accumulated on their lee side (Fig. 16G). Much of the coarse debris is buried or half-buried in a broader blanket of associated muddy sand, locally rich in pebbles. The patchy debris lobes contain scattered wooden poles and planks, aligned in a downslope direction or parallel to the lobe front and margins (Fig. 16B). Other anthropogenic litter, buried in the fine-grained sediment, includes rusty iron rods, cable pieces and tin cans.

The sedimentary features are typical of snow-avalanche deposits (Blikra & Nemec, 1998), which consist of coarse debris dragged along by a snowflow and a wider range of sediment that subsequently melted out from the emplaced snow mass. The blanket of fine-grained sediment, burying coarse debris, indicates incremental deposition from a large number of sediment-laden snowflows. In the upper part of sector 3, the debris-strewn surface shows a few parallel belts, several metres wide, nearly devoid of protruding debris, apparently swept clean by younger snowflows. The anthropogenic litter testifies to the recent age of the deposits and indicates that at least some of the snow avalanches descended from the vicinity of the old mine on the mountain slope (sector I*a* in Fig. 1B).

The outer bank of the active 'feeder' channel at its bend near the fan apex (Fig. 3A) has been markedly smoothed out by recent erosional stripping (Fig. 16A). This evidence indicates that the snow avalanches were descending the mountain slope along the channel and, by being considerably lighter than debrisflows, were spilling out by inertia at the channel bend, eroding the bank escarpment and turning it into an escape ramp. It is likely that some smaller or heavier, slushy snowflows failed to cross the ramp and came to rest on the channel floor, thus supplying additional meltwater and sediment to the stream in sector 2 during the summer.

The deposits in sector 3 indicate episodic accumulation of abundant snowdrift on the high catchment slope in modern times, perhaps as a result of occasional strong winds from the N or NE. Many of these large snow avalanches must have occurred after 1917 (when the local mine was established) and before 1936 (when the aerial photograph in Fig. 1B was taken). Some younger snowflows cannot be precluded, because this whole sector is still visibly fresh (Figs 13A and 16A), and much of the surficial debris bears no lichen (Fig. 16B–G).

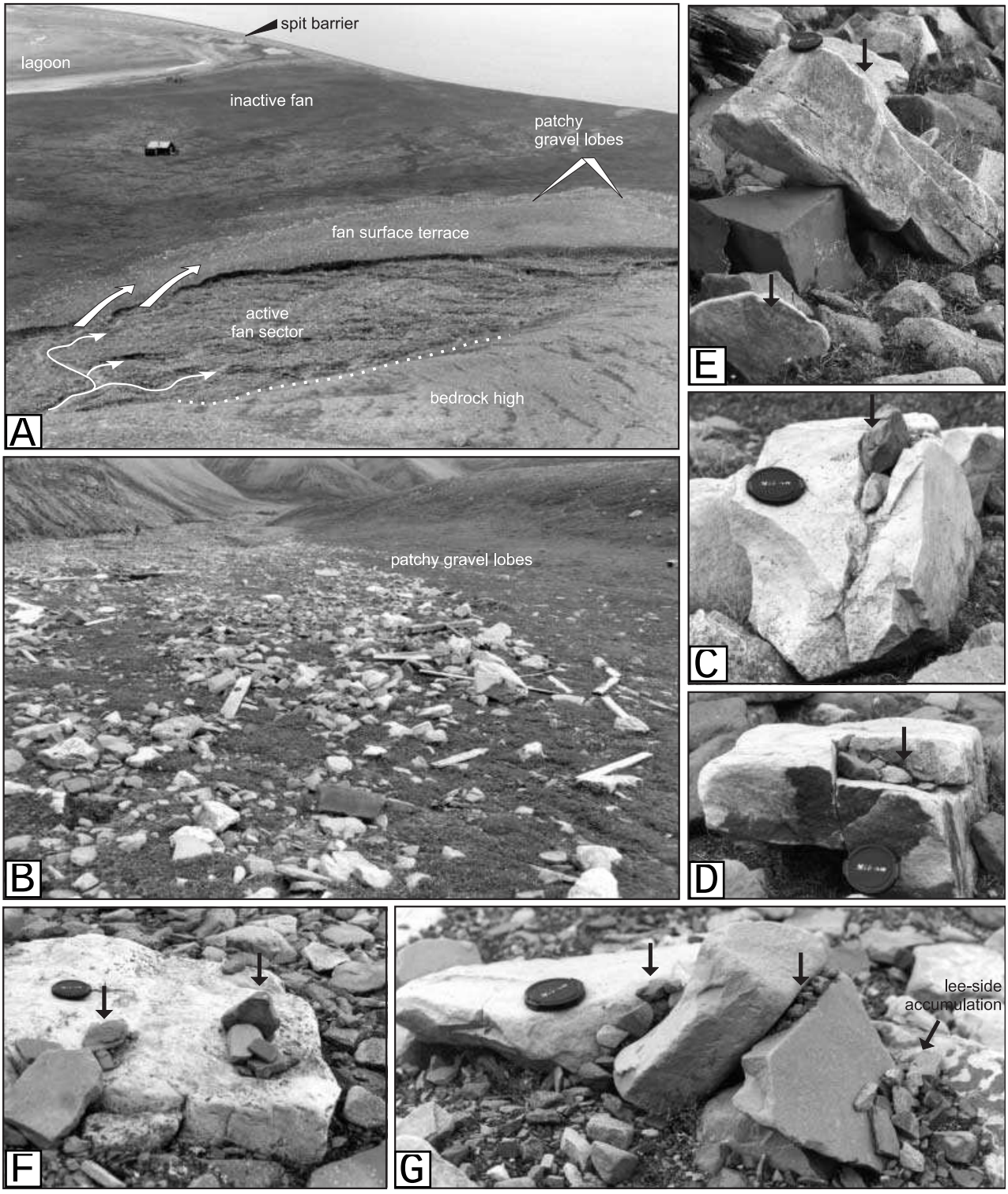

Active rockglacier in the catchment

A small rockglacier occupies the lower part of the cirque of Kiorthfjellet slope, extending from 550 m down to 370 m in altitude (see catchment sector II*a* in Fig. 1B). The cirque floor here is inclined at 35–45° (Fig. 2, profile A), and the surrounding slopes are even steeper, draped by an apron of colluvial deposits and shedding debris (Fig. 17A). The rockglacier is a tongue-shaped mound of immature gravel, ice-free at the surface, but internally filled with pore ice. The mound is

Fig. 16. (A) An oblique seaward view of the Hiorthfjellet fan delta in July 1999, showing the incised active sector 2 and the adjacent sector 3, where gravel has been deposited by modern snow avalanches on the raised surface of the inactive fan (cf. Fig. 13A). (B) The patchy gravel lobes deposited by snow avalanches in fan sector 3 (upfan view); note the angularity of unsorted debris, abundant boulders and the scattered wooden planks derived from the old mine on the mountain slope. The other photographs show close-up details. (C) Pebbles entrapped in an open fracture (arrow) at the top of a standing boulder. (D) A pocket of fine gravel (arrow) sheltered atop a boulder block. (E) Large clasts deposited in precarious positions; note the vertical disc-shaped cobble (lower arrow) and the steep rod-shaped boulder (upper arrow) leaning with its larger part on another, cube-shaped boulder. (F) Pockets of pebble gravel (arrows) perched precariously on a boulder block; downfan direction is away from the viewer. (G) Pockets of fine gravel (arrows) entrapped in the open spaces between clustered boulders; note the pebbles accumulated on the cluster lee side; downfan direction is to the right. The lens cap is 5 cm.

250 m in length and up to 100 m wide, thickening downslope and well adjusted to the cirque floor. It has a flat, downslope-inclined upper surface and a steep (36°) lobate front that is visibly fresh, nearly devoid of lichen, in its upper part (Fig. 17B and C). The front height and a 50-MHz ground-penetrating radar section (Isaksen *et al.*, 2000) indicate that the rockglacier is up to *c.* 40 m thick.

The creep of the rockglacier has exerted considerable drag on the adjoining talus apron on both sides, bending the colluvial rills and debris ridges in a downslope direction (Fig. 17B). The mean creep rate measured in 1994–97 is estimated to be in the range of 0·08–0·10 m year^{-1} (Isaksen *et al.*, 2000). The steepening-upward and fresh front reflects the collapsing of debris detached from its upper part during the summer thaw. The creep is apparently faster at upper levels, as is generally characteristic of slope creep processes (Blikra & Nemec, 1998) and rockglacier kinetics (Barsch, 1988, 1996; Haeberli & Vondermüll, 1996). The rockglacier surface in its northern upslope part bears little lichen and shows an array of swales and ridges reflecting asymmetrical creep and oblique subsurface drainage (Fig. 17B). The chevron ridges in the narrow root zone (Fig. 17B) are deposits of debrisflows derived from the cirque head slopes and accreted to the rockglacier rear flanks. The rockglacier is consistently replenished with slope-derived debris, as is typical in such geomorphic settings (André, 1994; Barsch, 1996; Berthling *et al.*, 1998).

The asymmetrical creep reflects active adjustment to the local topography and an effect of the cirque's oblique insolation, concentrated runoff and uneven yield of debris. The meltwater runoff is focused around the rockglacier, but is stronger and more erosive along its northern flank, where the cirque's south-facing slope yields more water. In the rockglacier forefront, the converging drainage routes are separated by a field of coarse, nearly openwork, water-washed gravel and merge further downslope into a single channel (Figs 1B and 17B).

The rockglacier is thought to have evolved from the ice-cored lateral moraines of a former cirque glacier. As the glacier melted, its moraine ridges lost support and began to creep on the steep slope, coalescing into a tongue-shaped mound. Based on the distance and rate of its movement, the rockglacier is estimated to have formed not earlier than 5·6 ka BP.

DISCUSSION

The evolution of the Hiorthfjellet fan delta and its catchment illustrates the character and many unique aspects of high-arctic sedimentation, and also has important implications for the history of Late Weichselian to Holocene regional deglaciation. The geological information derived from the sedimentary record is discussed below in terms of three major phases. The main chronological events recognized in the study area are summarized in Fig. 18 and are depicted as a series of interpretive palaeogeographical sketches in Fig. 19.

The late Weichselian to early Holocene phase

Near the end of the Weichselian, the Adventfjorden area was still occupied by the eastward-retreating ice front, which was here at least *c.* 1000 m thick, covering the local topography in excess of 900 m in present-day altitude (Fig. 19A). The U-shaped shallow depression at the crest of Hiorthfjellet (Fig. 1B) suggests an overspilling of ice from the adjacent valley, Mälardalen, probably coeval with the ice-front retreat from Adventfjorden. The fjord glacier was melting and thinning, exposing the higher part of Hiorthfjellet and causing an oblique westward runoff of meltwater across the plateau at 450 m altitude on the southern side of the fjord (Platåberget area in Fig. 1A). Adventfjorden was deglaciated around 10 ka BP, as is evidenced by the radiocarbon dates from a raised beach at 62 m

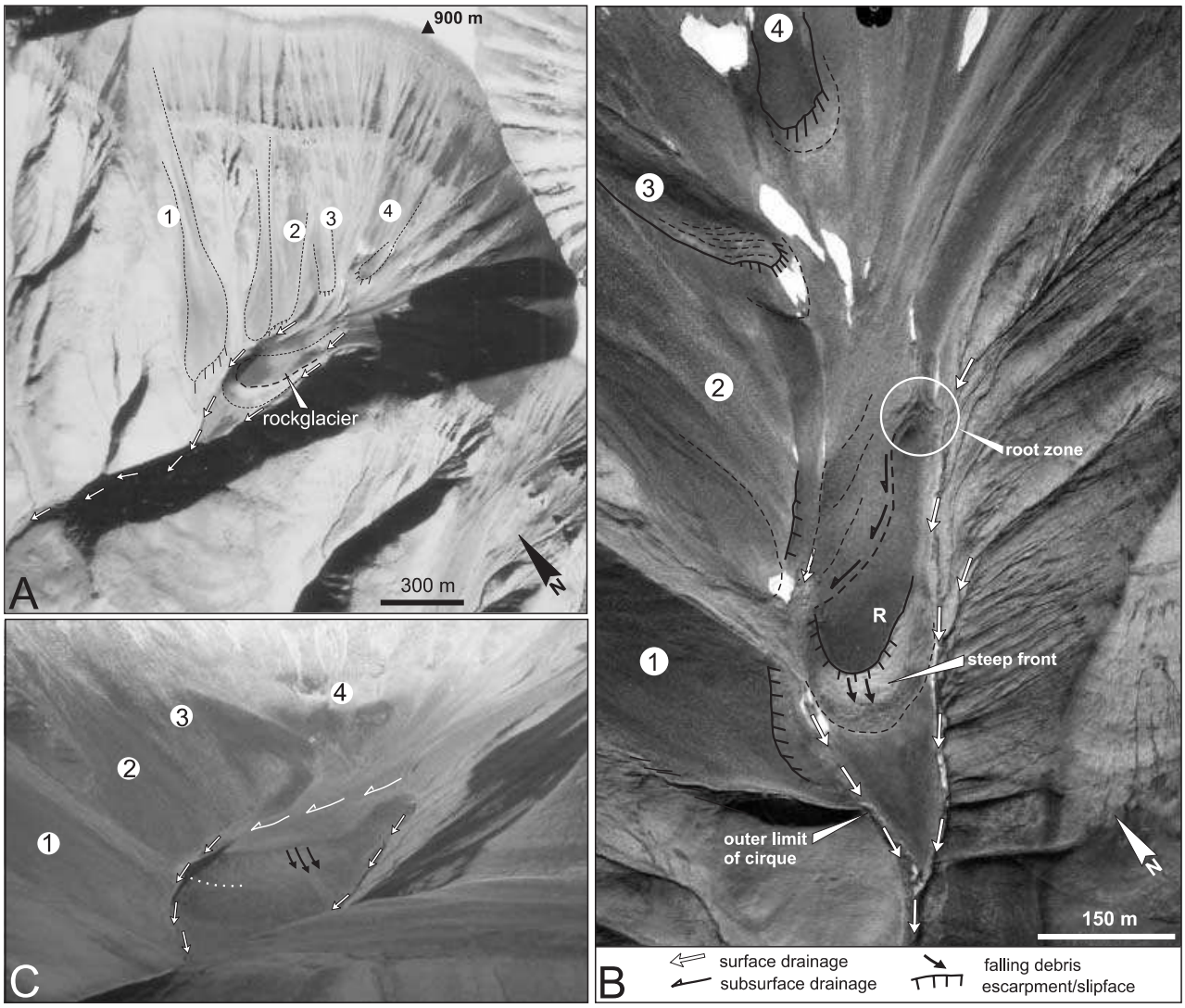

Fig. 17. (A) Portion of a vertical infrared aerial photograph (Norwegian Polar Institute, S90-5343) of the slope cirque (catchment sector II*a*, Fig. 1B), showing the active rockglacier surrounded by steep talus apron; the reference labels 1–4 indicate zones of pronounced sediment accumulation. (B) Detail from a vertical infrared aerial photograph (Norwegian Polar Institute, S95-1472) showing the tongue-shaped rockglacier (R) and the local morphology and drainage pattern. (C) Oblique photograph of the rockglacier, showing its steep front (with a relatively fresh upper, steepest part), the local pattern of water flow and the surrounding steep talus slopes.

altitude in Adventdalen, *c.* 16 km landwards from the fjord mouth (sample T-13882 in Table 1), and from raised marine deposits near the outlet of Blomsterdalen (Fig. 1A; T-11575 in Table 1). The tidewater glacier must have retreated quickly by calving from the deep fjord with a seaward-inclined floor free of topographic sills. The local marine limit is at an altitude of *c.* 70 m, beneath the apex of the Hiorthfjellet fan delta (Fig. 3A), which suggests that the latter commenced its development concurrently with the fjord deglaciation (Fig. 19B).

The catchment cirque morphology and evidence of abundant water and sediment supply to the fan delta indicate that the retreating Late Weichselian ice sheet left behind a small temperate glacier in the local slope niche, and that this isolated ice mass drove subglacial erosion and proglacial sedimentation. The high-arctic climate meant that the glacier was melted slowly, on a seasonal basis, protected by a cover of accumulating talus debris and snowdrift. It may also initially have been replenished with ice spilling over from Mälardalen, before the two ice masses became fully separated (Fig. 19B). The Hiorthfjellet slope may also have hosted some other, minor ice bodies, but these would have melted faster on the south-facing slope and yielded less water. Subglacial erosion in

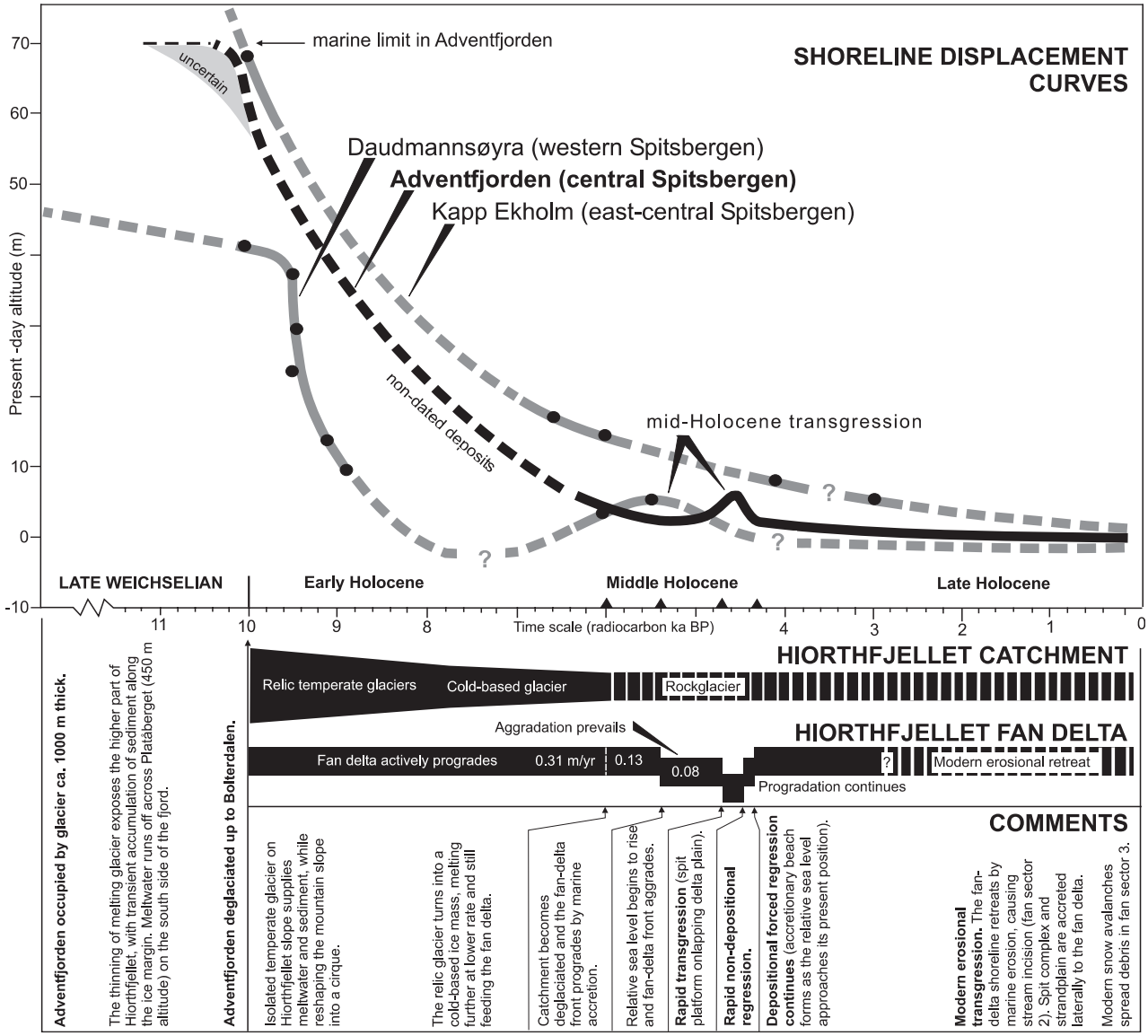

Fig. 18. The deglaciation history of the Adventfjorden area deciphered from the sedimentary record of the Hiorthfjellet fan delta and integrated with other relevant local and regional data. The shoreline displacement curve derived from the fan delta is hypothetical in its early Holocene part (no radiocarbon dates). It is compared with similar curves derived from raised beaches at Daudmannsøyra on the Spitsbergen west coast (modified from Forman, 1990) and Kapp Ekholm in inner Isfjorden (Salvigsen, 1984).

the cirque area declined as the melting glacier gradually decreased its thickness and basal pressure and turned into a cold-based ice body encompassed by the permafrost. The seasonal yield of meltwater persisted, with sediment supplied from the talus slopes and derived by erosion of the glacier's frontal moraine. The relative sea level in the fjord was falling (Fig. 18), as the regional glacioisostatic crustal uplift grossly outpaced the glacioeustatic sea-level rise. The highest activity of the fan delta thus coincided with a rapid forced regression.

The Gilbert-type fan delta prograded rapidly, at a mean rate of 0·31 m year^{-1} (Fig. 10), and reached a radius of nearly 1 km by *c.* 6 ka BP (Fig. 3A), while the relative sea level had concurrently fallen by 63 m (Fig. 4). The rate of relative sea-level fall thus averaged 0·016 m year^{-1}, but was gradually decreasing. Based on the fjord bathymetry (Figs 1A and 3A) and unpublished seismic data, the prograding fan delta is estimated to have reached a thickness of *c.* 25 m. The fan-delta volume was thus very large, compared with the catchment's small area and low present-day

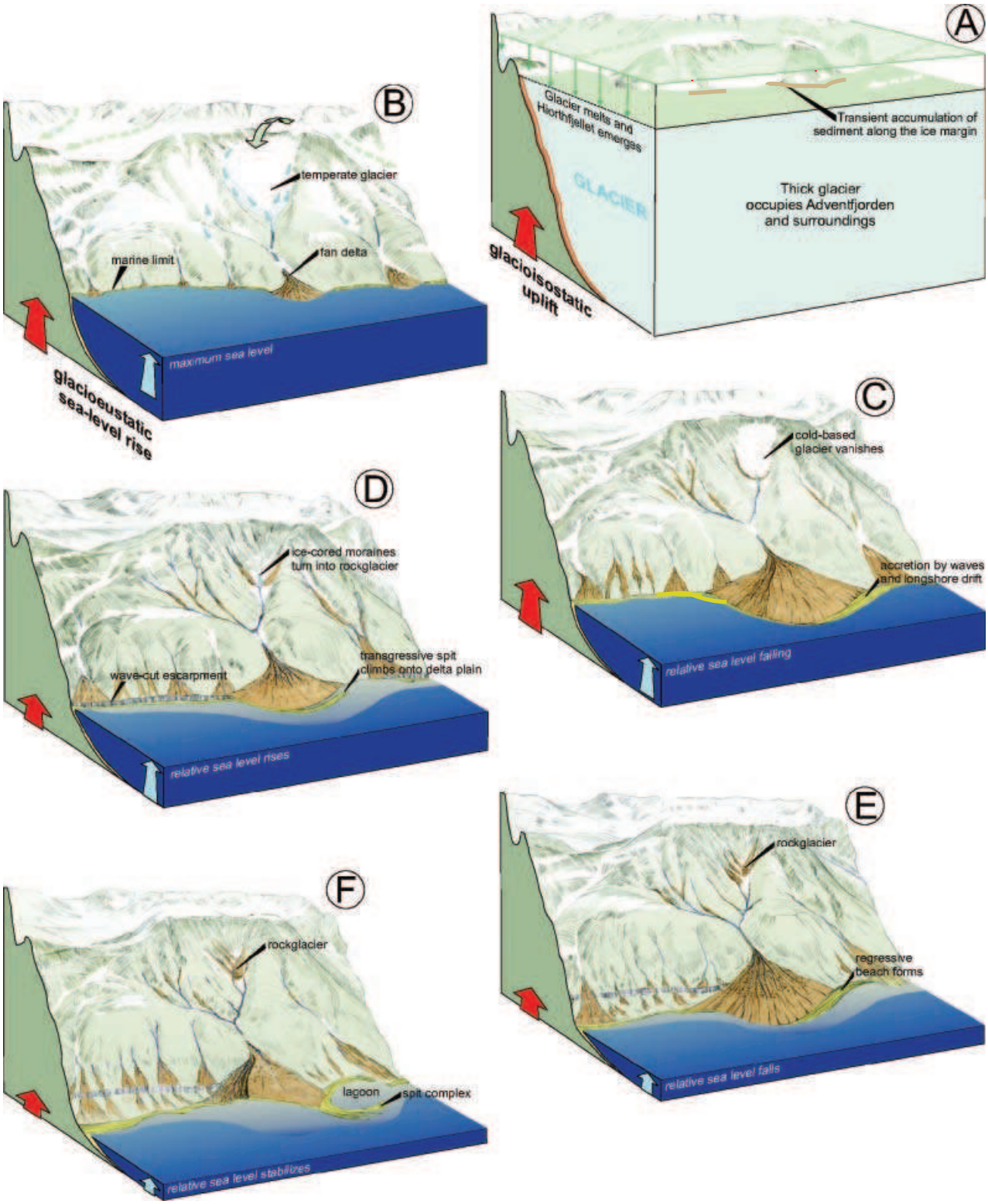

Fig. 19. The evolution of the Hiorthfjellet fan delta and its catchment, portrayed as a series of interpretive sketches (cf. Figs 1B and 18): (A) the Late Weichselian time; (B) the beginning of the Holocene; (C) the early Holocene; (D) the middle Holocene; (E) the end of the middle Holocene; and (F) the late Holocene. The events are discussed in the text.

water yield, which strongly supports the notion that the catchment remained glaciated until *c.* 6 ka BP, yielding abundant water and sediment.

The fan-delta foreset facies show the controlling role of sea waves, storms and tides, accompanied by slumping and beach-derived massflows, whereas mouth bars or other evidence of a direct subaqueous emplacement of stream-derived sediment are lacking. This relationship reflects a marked disequilibrium between the ephemeral stream discharges and strong wave action.

The activity of fluvial processes decreased markedly around 6 ka BP, when the alluvial fan ceased to advance and the rate of delta-front progradation decreased (Fig. 10). The decline in fluvial supply is attributed to the disappearance of the cirque glacier. The estimated time of the glacier demise is consistent with the independently estimated maximum age (*c.* 5·6 ka) of the successor rockglacier in the cirque catchment (Fig. 19D).

The middle Holocene phase

The relative sea level fell further by 5 m in 0·6 ka, which implies a much reduced rate, averaging 0·008 m year^{-1}. Despite the decline in fluvial supply, the fan-delta front had concurrently prograded by an additional 160 m (Fig. 4), notably in the eastern sector (Fig. 19C), increasing the subaerial delta plain to nearly 1·4 km^2 (Fig. 3A). This progradation was driven by wave action combined with sediment supply by longshore drift, and occurred at a considerably lower mean rate, estimated at 0·13 m year^{-1} (Fig. 10). The progradation rate decreased further to 0·08 m year^{-1} around 5·4 ka BP, when the relative sea level ceased to fall and probably began to rise slowly. In the eastern sector of the fan delta, the ensuing marine transgression was initially countered by longshore sediment supply, but this transient disequilibrium was also reversed by 4·7 ka BP (Fig. 10), when the delta-front beach rapidly aggraded and a transgressive spit began to climb onto the fan-delta plain (Fig. 4).

The gravelly spit platform climbed to a present-day altitude of *c.* 6 m (Figs 4 and 19D), recording a relative sea-level rise by 4 m (Fig. 18). The marine inundation reduced the radius of the fan-delta plain to 0·72 km and its area to 0·13 km^2. The wave-cut bedrock escarpment along the coast lateral to the fan delta, at an altitude of *c.* 6 m (Fig. 1B), was formed at this time (Fig. 19D). The subsequent forced regression was initially rapid and non-depositional, as the relative sea-level fall grossly outpaced fluvial sediment dispersal, while the shoreline of the re-emerging fan delta was being swept by longshore currents and not conducive to sediment accumulation. A regressive gravelly beach began to form around 4·3 ka BP, when the relative sea level had fallen to a present-day altitude of *c.* 1·7 m (Fig. 4) and began slowly to approach its present position (Figs 18 and 19E).

The mid-Holocene transgression in Adventfjorden, as recorded by the fan-delta deposits and constrained by radiocarbon dates to a time interval from 5·4 ka to *c.* 4·5 ka BP, was unrecognized by previous studies in central Spitsbergen. A mid-Holocene rise in relative sea level was recognized from raised beaches in the Nordenskiöldkysten area south of Isfjorden, on the Spitsbergen west coast, where it was estimated to have peaked at around 5·5 ka BP and reached a present-day altitude of up to 10 m (Landvik *et al.*, 1987). Similar evidence was found on the west coast north of Isfjorden, where the relative sea-level rise occurred between 6·5 ka and 5·0 ka BP and reached an altitude of 7 m (Forman, 1990). This mid-Holocene event is generally considered to have been diachronous, but was not recognized in either central Spitsbergen (Feyling-Hanssen, 1965; Salvigsen, 1984; see the Kapp Ekholm curve in Fig. 18) or the eastern part of Svalbard (Salvigsen, 1981). The present study indicates that the mid-Holocene transgression thus reached further eastwards than previously assumed.

The mid-Holocene transgression is attributed to a short-lived reversal of the imbalance between the rate of glacioisostatic crustal uplift and the rate of glacioeustatic sea-level rise. The post-glacial regional uplift was non-uniform and declined with time (Landvik *et al.*, 1998), reflecting the differential loading by the ice sheet and the decreasing rate of crustal rebound, which might explain the diachroneity and eastward decline of the event. However, the exact cause of this short-term reversal is not obvious and remains to be studied, taking into account its timing, high rates and magnitude. The mean rate of glacioeustatic sea-level rise is estimated at 13·6 m ka^{-1} for the period from 14 to 7 ka BP, later declining to 2·1 m ka^{-1} (Fairbanks, 1989), but there is also evidence of mid-Holocene fluctuations in sea level, on the order of 1–4·5 m and at apparent rates of 10–20 m ka^{-1} (Fairbridge, 1976, 1987; Colquhoun & Brooks, 1986; Colquhoun *et al.*, 1995). It is possible that one or more of

these fluctuations simply exceeded the regional rate of differential crustal uplift.

The late Holocene phase

The fan delta re-emerged as a result of the rapid fall in relative sea level (Fig. 18), increasing its area to 0·21 km^2 with a radius of 0·9 km (Fig. 19E). The fluvial distributary system, acting as a solitary channel, was wandering across the delta plain and occasionally extended to its outer margin across the exposed transgressive spit platform. The fan surface thus continued to aggrade slowly. The stream eventually shifted to the fan's low-lying northern flank and was entrapped there by incision, while the remainder of the fan surface was abandoned and subject to episodic sheetwash processes.

The abandoned fan-delta shoreline began to retreat by marine erosion, evolving into an escarpment, and the fluvial incision commenced as soon as the stream started to react to this new morphodynamic disequilibrium and adjust its own profile to the receding shoreline. The supply of sediment from the catchment continued, including debrisflows and debris-bearing sporadic snowflows. The ephemeral modern stream has been distributing this fresh sediment, with much difficulty, while degrading its profile further by substrate erosion. Short-term net aggradation often prevailed on a local scale, causing the stream to shift laterally and widen the active sector 2. The distal deposition of water-laid terminal splays over a laterally accreted strandplain (subsector 2a, Fig. 3A) is thought to reflect the increased accumulation of snow during the Little Ice Age maximum. The subsequent lateral expansion of the stream activity (subsector 2c) seems to have marked the onset of the modern conditions of seasonal snow accumulation. The active sector of the fan delta shows little recent progradation, for the stream discharges have long been incapable of competing with marine processes.

Marine processes have predominated along the shoreline in the late Holocene, as the relative sea level in Adventfjorden has gradually stabilized. The frontal part of the fan delta, eroded by waves, evolved into a wide shoal rimmed with a beach escarpment (Fig. 19F), which reduced the delta-plain area to *c.* 0·5 km^2 and a radius of little more than 0·6 km (Fig. 3A). The eroded sediment, swept by longshore drift, formed an accretionary spit complex that presently shelters the intertidal Moskuslaguna (Fig. 19F). The erosional transgression was accompanied by a progradational regression along the coast lateral to the fan delta, which reflects an inherited morphodynamic disequilibrium compensated actively by marine processes.

Modern snow avalanches have spread a blanket of debris in the head zone of the inactive fan (sector 3, Fig. 3A). Many of these large snowflows occurred between 1917 and 1936, some probably earlier and also later, which implies episodic abundant accumulation of snow on the high mountain slope in recent times.

CONCLUSIONS

The present study has reconstructed the history of a Holocene fan delta and its high-relief catchment in a deglaciated high-arctic fjord. Sedimentation processes in a freshly deglaciated terrain reflect widespread disequilibrium, referred to broadly as 'paraglacial' conditions (Church & Ryder, 1972). In a high-arctic climate, this transitional geomorphic regime is rather unusual, as it bears features of proglacial sedimentation and its duration is greatly extended (French, 1996). The development of fan deltas that followed the retreat of the last ice sheet from Svalbard has thus been controlled by a unique combination of physical conditions, including: a continued main role for meltwater, deriving from isolated relic glaciers, the permafrost active layer and winter snowpack; a seasonal pattern of meltwater and sediment supply; a strong impact of marine processes, interrupted by a winter lull when the coastal waters freeze over; and some very high rates of relative sea-level change.

The development of high-arctic coastal fans has been little explored, and their significance is unrecognized in specialized literature and textbook reviews. The present study serves to illustrate the character of high-arctic coastal sedimentation and demonstrates the importance of fan deltas as a proxy record of deglaciation history and environmental change in a high-arctic terrain. Fan deltas are highly sensitive recorders of environmental conditions (Nemec & Steel, 1988), for these systems straddle a crucial interface of environments, reflect the interplay of terrestrial and marine processes, respond to a wide range of disequilibria and are prone to rapid morphodynamic adjustments. Unlike large river deltas, they are products of local conditions, rather than a cumulative effect of extensive catchments. The resolution of a fan-deltaic record is also considerably higher than that of either an inland alluvium or a simple strand-

plain. The present case study of a fjord-side fan delta in central Spitsbergen allowed the deglaciation history of the fjord basin to be deciphered in unprecedented detail.

The study also has important regional implications. The current understanding of the deglaciation dynamics and climatic change in the region is based mainly on the offshore record. The scarcity of onshore glacigenic deposits misled geologists into assuming that the westward advance of the Late Weichselian ice sheet in Svalbard was chiefly limited to valleys and fjord heads, and that the western coasts and shelf of Svalbard were never covered by ice during the last glacial maximum. However, the modelling of regional crustal rebound has suggested that the ice sheet was at least 3000 m thick in the central part of the Barents Sea Shelf and probably as much as 800 m thick along the Svalbard west coast (Lambeck, 1995, 1996). The present study strongly supports this notion, because the glacier in the Adventfjord area in central Svalbard was apparently *c.* 1000 m thick.

The thinning ice sheet evolved into branching systems of tidewater glaciers, retreating rapidly by calving and shrinking into valley glaciers. However, the receding ice front on land left behind isolated glaciers in local topographic niches, and these ice bodies drove further subglacial erosion and proglacial sedimentation on a seasonal basis. It was these local 'drivers' that allowed the fan delta 'recorders' to form. The cirque glacier in the present case was supplying abundant water and sediment for up to 4000 years after the fjord deglaciation, although the glacier's location on the south-facing steep slope was hardly favourable for survival. The lifespan of the isolated relic glaciers varied, some of them surviving until the present time, and the local fan deltas should thus be regarded as an important record of the regional deglaciation dynamics and environmental change.

The study shows further that the mid-Holocene transgression, previously recognized only in western Svalbard (Landvik *et al.*, 1987; Forman, 1990), had a considerably wider eastward extent. The dynamics of this short-term fluctuation in relative sea level (its exact time span and magnitude and the rates of relative rise and fall) are little known, poorly constrained by radiocarbon data. The present study indicates that the relative sea level in Advantfjorden rose by 4 m in *c.* 900 years and then fell by more than 4 m in little more than 200 years, approaching its present-day position at a much lower and declining rate. The event here was thus brief and its rates were very high, with most of the relative sea-level change occurring at a rate of *c.* 0·02 m year^{-1}. However, it should be emphasized that the transgression was diachronous, controlled by the local rates of crustal rebound, and its regional dynamics remain to be analysed yet through local case studies.

ACKNOWLEDGEMENTS

The radiocarbon dating was done by the National Radiological Laboratory in Trondheim. Otto Salvigsen allowed an unpublished radiocarbon date of his sample T-11575 to be included, and the Norwegian Polar Institute kindly permitted publication of the aerial photographs. The manuscript was critically reviewed by I. Peter Martini and George Postma, and also benefited from editing by Peter Haughton and Michael Talbot.

REFERENCES

Åkerman, J. (1984) Notes on talus morphology and processes in Spitsbergen. *Geogr. Ann.*, **66A,** 267–284.

Allen, J.R.L. (1982) *Sedimentary Structures – Their Character and Physical Basis*, Vol. II. Developments in Sedimentology, 30b. Elsevier, Amsterdam, 663 pp.

André, M.-F. (1994) Rock glaciers in Svalbard: tentative dating and inferred long-term velocities. *Geogr. Ann.*, **76A,** 235–245.

Barsch, D. (1988) Rockglaciers. In: *Advances in Periglacial Geomorphology* (Ed. M.J. Clark), pp. 69–90. John Wiley & Sons, Chichester.

Barsch, D. (1996) *Rockglaciers: Indicators for the Present and Former Geoecology in High Mountain Environments*. Springer-Verlag, Berlin, 331 pp.

Berthling, I., Etzelmüller, B., Isaksen, K. and **Sollid, J.L.** (1998) Rock glaciers on Prins Karls Forland, Svalbard, I: Internal structure, flow velocity and morphology. *Permafr. Periglac. Proc.*, **9,** 135–145.

Blikra, L.H. and **Nemec, W.** (1998) Postglacial colluvium in western Norway: depositional processes, facies and palaeoclimatic record. *Sedimentology*, **45,** 909–959.

Bluck, B.J. (1999) Clast assembling, bed-forms and structure in gravel beaches. *Trans. Roy. Soc. Edinburgh Earth Sci.*, **89,** 291–332.

Boothroyd, J.C. and **Ashley, G.M.** (1975) Processes, bar morphology, and sedimentary structures on braided outwash fans, northeastern Gulf of Alaska. In: *Glaciofluvial and Glaciolacustrine Sedimentation* (Eds A.V. Jopling and B.C. McDonald), *SEPM Spec. Publ.*, **23,** 193–222.

Briseid, H.C. (1994) Sedimentology of a lacustrine gravelly palaeobeach in the Akarçay Basin, western Anatolia: sedimentary facies, processes and implications. Cand. Scient. Thesis, Bergen University.

Bull, W.B. (1977) The alluvial fan environment. *Prog. Phys. Geogr.*, **1,** 222–270.

Caldwell, N.E. and **Williams, A.T.** (1985) The role of beach profile configuration in the discrimination between differing depositional environments affecting coarse clastic beaches. *J. Coast. Res.*, **1,** 129–139.

Carter, R.W.G., Orford, J.D., Forbes, D.L. and **Taylor, R.B.** (1990) Morphosedimentary development of drumlin–flank barriers with rapidly rising sea level, Story Head, Nova Scotia. *Sed. Geol.*, **69,** 117–138.

Church, M. and **Jones, D.** (1982) Channel bars in gravel-bed rivers. In: *Gravel-Bed Rivers* (Eds R.D. Hey, J.C. Bathurst and C.R. Thorne), pp. 83–105. John Wiley & Sons, Chichester.

Church, M. and **Ryder, J.M.** (1972) Paraglacial sedimentation: a consideration of fluvial processes conditioned by glaciation. *Geol. Soc. Am. Bull.*, **83,** 3059–3072.

Colella, A. and **Prior, D.B.** (eds) (1990) Coarse-grained deltas. *Int. Assoc. Sedimentol. Spec. Publ.*, **10,** 357 pp.

Colquhoun, D.J. and **Brooks, M.J.** (1986) New evidence from the southeastern US for eustatic components in the late Holocene sea levels. *Geoarchaeology*, **1,** 275–291.

Colquhoun, D.J., Brooks, M.J. and **Stone, P.A.** (1995) Sea-level fluctuations: emphasis on temporal correlations with records from areas with strong hydrologic influences in the southeastern United States. In: *Holocene Cycles* (Ed. C.W. Finkl, Jr), *J. Coastal Res.*, Spec. Issue, 191–196.

Dallman, W.K., Kjærnet, T. and **Nøttvedt, A.** (2001) *Geological Map of Svalbard 1:100 0000, Sheet C9G, Adventdalen.* Norwegian Polar Institute, Tromsø.

Dixon, J.C. and **Abrahams, A.D.** (eds) (1992) *Periglacial Geomorphology.* John Wiley and Sons, Chichester.

Elverhøi, A., Svendsen, J.I., Solheim, A., Andersen, E.S., Milliman, J.D., Mangerud, J. and **Hook, LeB.R.** (1995) Late Quaternary sediment yield from the high arctic Svalbard area. *J. Geol.*, **103,** 1–17.

Fairbanks, R.G. (1989) A 17,000-year glaci-eustatic sea level record: influence of glacial melting rates on the Younger Dryas event and deep ocean circulation. *Nature*, **342,** 637–642.

Fairbridge, R.W. (1976) Shellfish-eating perceramic Indians in coastal Brasil. *Science*, **191,** 353–359.

Fairbridge, R.W. (1987) The spectra of sea level in a Holocene time frame. In: *Climate, History, Periodicity and Predictability* (Eds M.R. Rampino, J.E. Sanders, W.S. Newman and L.K. Kingsson), pp. 127–112. Van Nostrand, New York.

Feyling-Hanssen, R. (1965) Shoreline displacement in central Vestspitsbergen and a marine section from the Holocene of Talavera on Barentsøya in Spitsbergen. *Nor. Polarinst. Meddel.*, **93,** 34 pp.

Fitzgerald, D.M., Penland, S. and **Nummedal, D.** (1984) Control of barrier island shape by inlet sediment bypassing: East Frisian Islands, West Germany. *Mar. Geol.*, **60,** 355–376.

Folk, R.L. (1974) *Petrology of Sedimentary Rocks.* Hemphill, Austin, TX, 170 pp.

Førland, E.J., Hanssen-Bauer, I. and **Nordli, P.Ø.** (1997) Climate statistics and longterm series of temperature and precipitation at Svalbard and Jan Mayen. *Norw. Meteorol. Inst. Report*, **21/97,** 72 pp.

Forman, S.L. (1990) Post-glacial relative sea-level history of northwestern Spitsbergen, Svalbard. *Geol. Soc. Am. Bull.*, **102,** 1580–1590.

French, H.M. (1996) *The Periglacial Environment*, 2nd edn. Longman, Harlow, 341 pp.

Gjessing, Y., Hagen, J.O., Hassel, K.A., Sand, K. and **Wold, B.** (eds) (1990) *Arctic Hydrology: Present and Future Tasks.* Norw. Natl. Commit. Hydrol. Report, 23, pp. 139–146.

Gruszczyński, M., Rudowski, S., Semil, J., Skomiński, J. and **Zrobek, J.** (1993) Rip currents as a geological tool. *Sedimentology*, **40,** 217–236.

Haeberli, W. and **Vondermüll, D.** (1996) On the characteristics and possible origins of ice in rock glacier permafrost. *Z. Geomorph. Suppl. Bd.*, **104,** 43–57.

Hiroki, Y. and **Masuda, F.** (2000) Gravelly spit deposits in a transgressive systems tract: the Pleistocene Higashikanbe Gravel, central Japan. *Sedimentology*, **47,** 135–149.

Hobday, D.K. and **Banks, N.L.** (1971) A coarse grained pocket beach complex, Tanafjord (Norway). *Sedimentology*, **16,** 129–134.

Isaksen, K., Ødegård, R.S., Eiken, T. and **Sollid, J.L.** (2000) Composition, flow and development of two tongue-shaped rock glaciers in the permafrost of Svalbard. *Permafr. Periglac. Proc.*, **11,** 241–257.

Jahn, A. (1960) Some remarks on evolution of slopes on Spitsbergen. *Z. Geomorph., Suppl. Bd.*, **1,** 49–58.

Jahn, A. (1967) Some features of mass movement on Spitsbergen slopes. *Geogr. Ann.*, **49A,** 213–225.

Johansen, T.A., Digranes, P., Van Schaack, M. and **Lønne, I.** (2003) On seismic mapping of shallow sediments in polar areas. *Geophysics*, **68,** 566–573.

Komar, P.D. (1976) *Beach Processes and Sedimentation.* Prentice Hall, Englewood Cliffs, NJ, 417 pp.

Koster, E.H. (1978) Transverse ribs: their characteristics, origin and paleohydraulic significance. In: *Fluvial Sedimentology* (Ed. A.D. Miall), *Can. Soc. Petrol. Geol. Mem.*, **5,** 161–186.

Kraft, J.C., Allen, E.A. and **Maurmeyer, E.M.** (1978) The geological and paleogeomorphological evolution of a spit system and its associated coastal environments: Cape Henlopen Spit, Delaware. *J. Sed. Petrol.*, **48,** 211–226.

Lægreid, A.K. (1999) Postglacial sedimentation in a high-arctic valley: slope processes and geomorphic development in Endalen, Spitsbergen. Cand. Scient. Thesis, Bergen University, 134 pp.

Lambeck, K. (1995) Constraints on the Late Weichselian ice sheet over the Barents Sea in Late Weichselian time. *Quatern. Sci. Rev.*, **14,** 1–16.

Lambeck, K. (1996) Limits on the areal extent of the Barents Sea ice sheet in Late Weichselian time. *Global Planet. Change*, **12,** 41–51.

Landvik, J.Y., Mangerud, J. and **Salvigsen, O.** (1987) The Late Weichselian and Holocene shoreline displacement on the west-central coast of Svalbard. *Polar Res.*, **5,** 29–44.

Landvik, J.Y., Bondevik, S., Elverhøi, A., Fjeldskaar, W., Mangerud, J., Siegert, M.J., Salvigsen, O., Svendsen, J.I. and **Vorren, T.O.** (1998) The last glacial maximum of Svalbard and the Barents Sea area: ice sheet extent and configuration. In: *Glacial and Oceanic History of the Polar North Atlantic Margins* (Eds A. Elverhøi, J. Dowdeswell, S. Funder, J. Mangerud and R. Stein), *Quatern. Sci. Rev.*, **17,** 43–75.

Larsson, S. (1982) Geomorphological effects on the slopes of Longyear valley, Spitsbergen, after a heavy rainstorm in July 1972. *Geogr. Ann.*, **64A,** 105–125.

Liestøl, O. (1976) Pingos, springs and permafrost in Spitsbergen. *Nor. Polarinst. Årbok*, **1975,** 7–29.

Lønne, I., Nemec, W., Blikra, L.H. and **Lauritsen, T.** (2001) Sedimentary architecture and dynamic stratigraphy of a marine ice-contact system. *J. Sed. Res.*, **71,** 924–945.

Lowe, D.R. (1982) Sediment gravity flows, II. Depositional models with special reference to the deposits of high-density turbidity currents. *J. Sed. Petrol.*, **52,** 279–297.

Lysså, A. and **Lønne, I.** (2001) Moraine development at a small high-arctic valley glacier: Rieperbreen, Svalbard. *J. Quatern. Sci.*, **16,** 519–529.

Major, H., Nagy, J., Haremo, P., Dallmann, W.K. and **Andresen, A.** (2000) *Geological Map of Svalbard, 1:100 000, Sheet C9G*. Norwegian Polar Institute, Tromsø.

Mangerud, J., Dokken, T., Hebbeln, D., Heggen, B., Ingólfsson, Ó., Landvik, J.Y., Mejdahl, V., Svendsen, J.I. and **Vorren, T.** (1998) Fluctuations of the Svalbard-Barents Sea Ice Sheet during the last 150 000 years. In: *Glacial and Oceanic History of the Polar North Atlantic Margins* (Eds A. Elverhøi, J. Dowdeswell, S. Funder, J. Mangerud and R. Stein), *Quatern. Sci. Rev.*, **17,** 11–42.

Massari, F. (1996) Upper-flow-regime stratification types on steep-face, coarse-grained, Gilbert-type progradational wedges (Pleistocene, southern Italy). *J. Sed. Res.*, **66,** 364–375.

Massari, F. and **Parea, G.C.** (1988) Progradational gravel beach sequences in a moderate- to high-energy microtidal marine environment. *Sedimentology*, **35,** 881–913.

Mount, J.F. and **Kidder, D.** (1993) Combined-flow origin of edgewise intraclast conglomerates: Sellick Hill Formation (Lower Cambrian), South Australia. *Sedimentology*, **40,** 315–329.

Nemec, W. (1990) Aspects of sediment movement on steep delta slopes. In: *Coarse-Grained Deltas* (Eds A. Colella and D.B. Prior), *Int. Assoc. Sedimentol. Spec. Publ.*, **10,** 29–73.

Nemec, W. (1995) The dynamics of deltaic suspension plumes. In: *Geology of Deltas* (Eds M.N. Oti and G. Postma), pp. 31–93. A.A. Balkema, Rotterdam.

Nemec, W. and **Postma, G.** (1993) Quaternary alluvial fans in southwestern Crete: sedimentation processes and geomorphic evolution. In: *Alluvial Sedimentation* (Eds M. Marzo and C. Puigdefábregas), *Int. Assoc. Sedimentol. Spec. Publ.*, **17,** 235–276.

Nemec, W. and **Steel, R.J.** (eds) (1988) *Fan Deltas – Sedimentology and Tectonic Settings*. Blackie, London, 444 pp..

Nemec, W., Lønne, I. and **Blikra, L.H.** (1999) The Kregnes moraine in Gauldalen, west-central Norway: anatomy of a Younger Dryas proglacial delta in a palaeofjord basin. *Boreas*, **28,** 454–476.

Nicholls, R.J. and **Webber, N.B.** (1987) The past, present and future evolution of Hurst Castle Spit, Hampshire. *Prog. Oceanogr.*, **18,** 119–137.

Nilsen, T.H. and **Moore, T.E.** (1984) *Bibliography of Alluvial-Fan Deposits*. Geo Books, Norwich, 96 pp.

Postma, G. and **Cruickshank, C.** (1988) Sedimentology of a late Weichselian to Holocene terraced fan delta, Varangerfjord, northern Norway. In: *Fan Deltas – Sedimentology and Tectonic Settings* (Eds W. Nemec and R.J. Steel), pp. 144–157. Blackie, London.

Postma, G. and **Nemec, W.** (1990) Regressive and transgressive sequences in a raised Holocene gravelly beach, southwestern Crete. *Sedimentology*, **37,** 907–920.

Rachocki, A.H. and **Church, M.** (eds) (1990) *Alluvial Fans: a Field Approach*. John Wiley & Sons, Chichester, 301 pp.

Rapp, A. (1960) Talus slopes and mountain wall at Tempelfjorden, Spitsbergen: a geomorphological study of the denudation of slopes in an arctic locality. *Nor. Polarinst. Skr.*, **119,** 1–96.

Rudberg, S. (1986) Present-day geomorphological processes on Prins Oscars Land, Svalbard. *Geogr. Ann.*, **68A,** 41–63.

Rudberg, S. (1988) High arctic landscapes: comparison and reflections. *Nor. Geogr. Tidsskr.*, **42,** 255–264.

Sallenger, A.H., Jr (1979) Inverse grading and hydraulic equivalence in grainflow deposits. *J. Sed. Petrol.*, **49,** 553–562.

Salvigsen, O. (1981) Radiocarbon dated raised beaches in Kong Karls Land, Svalbard, and their consequences for the glacial history of the Barents Sea. *Geogr. Ann.*, **63A,** 280–291.

Salvigsen, O. (1984) Occurrence of pumice on raised beaches and Holocene shoreline displacement in the inner Isfjorden area, Svalbard. *Polar Res.*, **2** (n.s.), 107–113.

Salvigsen. O., Forman, S. and **Miller, G.** (1992) Thermophilous molluscs on Svalbard during the Holocene and their paleoclimatic implications. *Polar Res.*, **11,** 1–10.

Sepkoski, J.J. (1982) Flat-pebble conglomerates, storm deposits, and the Cambrian bottom fauna. In: *Cyclic and Event Stratification* (Eds G. Einsele and A. Seilacher), pp. 371–385. Springer-Verlag, Berlin.

Sherman, D.J., Orford, J.D. and **Carter, R.W.G.** (1993) Development of cusp-related, gravel size and shape facies at Malin Head, Ireland. *Sedimentology*, **40,** 1139–1152.

Sletten, K., Lysså, A. and **Lønne, I.** (2001) Formation and disintegration of a modern high arctic ice-contact system, Scott Turnerbreen, Svalbard. *Boreas*, **30,** 272–284.

Smith, N.D., Phillips, A.C. and **Powell, R.D.** (1990) Tidal drawdown: a mechanism for producing cyclic sediment laminations in glaciomarine deltas. *Geology*, **18,** 10–13.

Soltvedt, S. (2000) *Postglacial sediment transport in Endalen, Svalbard*. Cand. Scient. Thesis, Bergen University, 144 pp.

Svendsen, J.I. and **Mangerud, J.** (1992) Paleoclimatic inferences from glacial fluctuations on Svalbard in the last 20,000 years. *Climate Dynam.*, **6,** 213–220.

Svendsen, J.I. and **Mangerud, J.** (1997) Holocene glacial and climatic variations on Spitsbergen, Svalbard. *Holocene*, **7,** 45–57.

Svendsen, J.I., Elverhøi, A. and **Mangerud, J.** (1996) The retreat of the Barents Sea ice sheet on western Svalbard margin. *Boreas*, **25,** 244–256.

Vorren, T.O., Laberg, J.S., Blaumme, F., Dowdeswell, J.A., Kenyon, N.H., Mienert, J., Rumohr, J. and **Werner, F.** (1998) The Norwegian-Greenland Sea continental margins: morphology and Late Quaternary sedimentary processes and environment. In: *Glacial and Oceanic History of the Polar North Atlantic Margins* (Eds A. Elverhøi, J. Dowdeswell, S. Funder, J. Mangerud and R. Stein), *Quatern. Sci. Rev.*, **17,** 273–302.

Wasson, R.J. (1977) Catchment processes and the evolution of alluvial fans in the lower Derwent valley, Tasmania. *Z. Geomorph. N.F.*, **21,** 147–168.

Whisonant, R.C. (1987) Paleocurrent and petrographic analysis of imbricate intraclasts in shallow-marine carbonates, Upper Cambrian, southwestern Virginia. *J. Sed. Petrol.*, **57,** 983–994.

Williams, A.T. and **Caldwell, N.E.** (1988) Particle size and shape in pebble-beach sedimentation. *Mar. Geol.*, **82,** 199–215.

Manuscript received 25 January 2003;
revision accepted 14 January 2004.